Underneath the surface

Advanced synchrotron techniques for the study of 17th century oil paint in three dimensions

Broers, F.T.H.

Publication date
2025

1

Introduction

"... arts and sciences are branches of the same tree."
- Albert Einstein (1937)

Oil paintings displayed in museums often give the impression of eternity. These, often centuries-old, works of art serve as symbols of our cultural heritage. However, preserving these masterpieces for future generations requires meticulous care. Nowadays, museums employ climate control systems, controlled lighting and other conservation measures to create an environment far more favorable to the preservation of art than in past centuries.[1,2] To ensure the long-term preservation of these artworks, a thorough understanding of the paintings' material composition and degradation, as well as the original intentions of the artist is necessary to comprehend the behavior of the material. We need to fully understand the complex objects, from the varnished surface down to the canvas, from the macroscale down to the nanoscale.

Chemically, oil paintings are far from the static, two-dimensional objects they are perceived to be by the casual onlooker. Over time, the paintings are subjected to a range of internal processes and external factors that can alter their appearance and composition. The true 'original' version of an oil painting may exist only at the precise moment the artist completed it. Even then, the painting would have already undergone chemical changes during the making process. Oil paintings involve multiple distinct layers of paint that each may consist of a wide variety of both organic and inorganic components. Once paint is applied, chemical reactions, starting with the chemical drying process of oil paint, are initiated and continue over centuries. Degradation phenomena, such as discoloration of pigments[3], flaking or delamination of paint layers[4,5], or the formation of lead soap protrusions[6], are common. Physical alterations, such as craquelure formation, further contribute to the transformation of paintings over time.

To understand all aspects of an oil painting – its creation, its composition, its degradation, its current condition, and the best way to treat and preserve it – research is needed. Throughout the years, various analytical techniques have been used to study oil paintings. This type of research often starts using non-invasive scanning techniques, but to study the complex stratigraphy and composition of paint systems, using microscale techniques on paint samples is crucial. In this thesis, different three dimensional micro- and nanoscale chemical analysis techniques are used to explore and evaluate what these techniques can contribute to the understanding of 17th century oil paintings and their degradation. These techniques include full field transmission X-ray microscopy (FF-TXM) and correlated X-ray fluorescence and ptychographic tomography. Most of the research was performed at synchrotron light source facilities, by bringing micrometric sized paint samples that are almost 400 years old to these state-of-the-art research institutions.

1.1 Three-dimensionality of oil paintings

A schematic overview of the stratigraphy of a 17th century oil painting is shown in **Figure 1.1**. The support (layer (1) in **Figure 1.1**) of a painting is typically a stretched canvas or wooden panel, but other supports such as copper plates were used as well.[7] The support is then covered with one or multiple preparatory layer(s) (2). The most commonly applied method in the 17th century was an animal glue sizing. This layer evens the surface and prevents the oil from the later applied oil paint to get absorbed by the canvas. Further preparation of the support was done by applying one or multiple ground layers (3). These ground layers, with a variety in color and material[7], made sure that the painter had a smooth and even surface to paint on. From this point, artists would sometimes choose to sketch (part of) the composition on the prepared canvas, which we call an underdrawing (4). The next layer consists of one

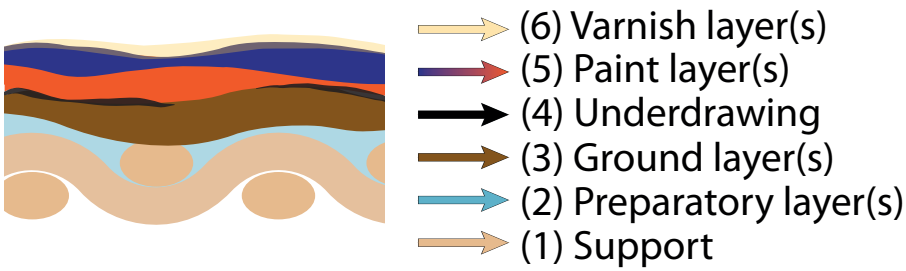

Figure 1.1. General schematic representation of the different layers of a 17th century oil painting.

or multiple paint layers (5). Finally, a painting was usually completed by applying a varnish layer (6) to protect the paint as well as to saturate the colors. This varnish layer is removed and re-applied at intervals by conservators due to its yellowing over time. In the underlying paint layers, next to the original materials, materials of past conservation treatments can be found. For example, if an area has endured damage, such as small or larger paint losses, these damages might have been treated in the past by filling the lacunae and by applying 'overpaint'. It can be necessary for the conservator to remove the old fill material and overpaint, and to assess whether and how to reapply these.[7]

The complex stratigraphy and three-dimensionality of paintings is one of the reasons why during a research and conservation project of a painting, sometimes small paint samples are taken. The samples are typically taken after non-invasive research was performed on the painting, allowing for specific areas of the artwork to be examined to address further questions. The size of these micro paint fragments often corresponds to the diameter of one or a few human hairs (50 - 500 µm). They are carefully taken by a conservator which removes them from the painting using a scalpel, preferably in an area where there was already some damage to the paint surface, for example along the edges of craquelures. To study the stratigraphy of the paint and to be able to safely handle these precious micro samples, they are embedded in small resin blocks. By polishing these along the stratigraphy, a paint cross section is obtained.[8]

All the different organic and inorganic materials present in the stratigraphy make paintings a - chemically - very heterogenous material. Paint is a mixture of a pigment and a binder. The pigment is what defines the color, and the binder holds the pigment particles in place. From the 15th century onwards, binders such as tempera (mixture of egg yolk, water and/or animal glue) and gum Arabic were gradually replaced by drying oils.[9,10] The drying oil that was used most in the 17th century was linseed oil, but also other oils such as poppy seed or walnut oil were employed.

Drying oils are oils that dry not due to a physical, moisture evaporation driven process, but due to complex polymerization reactions involving oxygen from the atmosphere and unsaturated bonds within the fatty acid molecules of the oil.[11] Drying oils consist of triacyl glycerides (TAGs). These esters consist of a glycerol component and three fatty acids. The fatty acids in TAGs can be fully saturated or have one to three unsaturated bonds. In case of a drying oil, a large number of unsaturated bonds is favorable for the cross-linking and polymerization reactions to cure the oil.[12,13] The oils used as binder in the 17th century were all natural products and the exact composition and ratio between fatty acids can differ. The polymerization process transforming a liquid oil into a solid film consists of many steps and has an almost infinite

number of possible pathways due to the different fatty acids present and the many unsaturated bonds that can react in different sequences. The hardening of oil is an autoxidation process, initiated by a reactive bis-allylic radical (hydrogen from a carbon positioned in-between two non-conjugated double bonds is extracted). Atmospheric oxygen can react with these radicals, forming (very reactive) hydroperoxide groups. After this initiation, the propagation phase starts. In this phase, multiple different chemical reactions are competing such as cross-linking between TAGs but also oxidation and chain scission. Termination of the process takes place when two radicals meet.[11,14,13,15] A schematical overview of the chemical reactions taking place can be found in the study by DePolo *et al.*[15]

Next to the chemically active organic binder, the pigments and driers added to the paint are also the cause for a wide variety of chemical reactions in paintings. Many pigments and driers consist of one or more metals, such as lead, arsenic or cobalt. Lead driers are added to oil to catalyze its drying process.[16] All of these metals, especially in ionic form, can cause or participate in chemical reactions. The presence of cations such as zinc, lead or copper, can cause a reaction with the binder and result in an ionomer-like network.[12,14,17,18] This can increase the stability of the paint film[18], but can also cause the formation of metal soaps.[17] Degradation of the pigment itself often manifests itself as a color loss or color change. The same pigment can degrade via different pathways depending on the local conditions. The pigments, drying oil, the presence of water and light or temperature are all part of the local conditions in a painting. When the chemical reactions cause a change in the material, for example a color loss of a pigment or a new product forming within the paint, we call these degradation phenomena. Section 1.5 discusses some of the most prevalent pigments and the related degradation phenomena in this thesis.

1.2 2D macro- and micro-imaging

To study the creation, composition, degradation, and the current condition of paintings, a wide variety of techniques are used. The field of heritage or conservation science has undergone a lot of development and innovations in the last decades. A distinction is typically made between investigations on the macroscale and analyses on the microscale. The former refers to analytical methods used directly on the object as a whole, and the latter refers to analytical research performed on small samples taken from the object. In this section, we will focus on the most commonly used macro and micro-imaging methods, disregarding single spot measurements.

1.2.1 Macroscale

X-ray radiography has been used since the end of the 19th century, only a year after the discovery of X-rays, to inspect paintings.[19] X-ray radiography is an important tool to examine paintings, as it is a relative accessible technique and can provide many insights for a researcher or conservator. The greyscale contrast in an X-ray radiograph shows the level of X-ray absorbance by the material it penetrates. Dense materials – such as iron nails or lead white paint – strongly absorb X-rays and show up as white, while organic materials such as a varnish absorb less and show up dark in a radiograph. With this technique often alterations in the painting (either during the creative process or as later retouches) and painting technique can be visualized. Similarly, **infrared reflectography** (IRR) and **photography** (IRP) enable us to look beneath the surface of a painting. IRR was developed at the end of the 1960s and one of the main advantages is that (dark) underdrawings can be visualized.[20–22] Ultraviolet

(UV) light sources are used to investigate the fluorescence observed in paintings. Often, the **UV fluorescence** is recorded by photography, and this is used as documentation of the condition of the painting, along with the aforementioned methods. The most common goal of using UV fluorescence is to study the spatial distribution of the varnish on a painting. Most used varnishes naturally exhibit molecular fluorescence. The emission maximum of the fluorescence of the varnish changes with time; thus, by studying the differences in intensity at a certain wavelength, restorations can often be identified. A stronger fluorescence can also identify a thicker layer or multiple layers of varnish.[23]

Macroscale X-ray fluorescence (MA-XRF) is one of the most influential macroscale techniques of the past decade. The development of (commercially available) MA-XRF scanners allow elemental mapping analysis of entire paintings. This technique enables to distinguish and visualize the different elements present in a painting. Whereas the data of an X-ray radiograph can be considered to provide a two-dimensional result (one greyscale image), in the case of MA-XRF, we obtain a three-dimensional data cube, comprised of a series of images at different energies. By performing a fit of the data using a mathematical model, element distribution maps can be obtained.[24–28] The probing depth of MA-XRF depends on the attenuation of X-rays by the materials in the painting and can be either several micrometers or all the way to the canvas.[29,30] Scans are collected in reflectance mode, and the signal from low Z elements in the deeper layers of the painting is often reabsorbed by layers above it, especially if these are e.g. lead-based materials. The resolution of MA-XRF scans depends on the available scanning time, but usually between 150 and 500 µm.

Another informative technique to study paintings at the macroscale is **reflectance imaging spectroscopy** (RIS). This method was previously often called hyperspectral imaging. RIS provides molecular information. Multiple imaging spectrometers or hyperspectral cameras are used to measure the interaction of light and matter across different ranges of the electromagnetic spectrum. To collect a full RIS data set, at the Rijksmuseum two cameras are used, one camera collecting the visible to near infrared (VNIR) from 400 to 1000 nm and the other camera collecting the short wave infrared (SWIR) from 900 to 2500 nm.[31] A three-dimensional data cube is collected, in which a reflectance spectrum corresponds to every pixel of the x-y-plane. Collected spectra can be compared to the fingerprints of different molecules and therefore allow for the identification of pigments. Once pigments are identified, the related spectra (so called endmembers) can provide distribution maps, corresponding to the surface of the painting, by using specific mapping algorithms. In the VNIR part, mostly information on pigments present in the visible paint layers is contained, as the visible spectral region gives information about electronic transition and therefore colors and has a maximum of 50 micrometer penetration depth. The SWIR part of the spectrum has a higher penetration depth and comprises information from deeper lying layers of the painting and –depending on the attenuation of materials in the upper layers – can penetrate all the way to the canvas.
To better visualize changes in composition, sketches made by the artist, and to have a first separation of materials reacting differently to the light, false color images are usually created with the SWIR dataset. Three infrared wavelengths are substituted to the red green and blue channel (of a common RGB) to create a false color infrared image.[32–35] The spatial resolution of RIS can vary depending on the imaging spectrometer (commonly from 100 µm to 1 mm). Usually both VNIR and SWIR are kept at similar spatial resolution between 150 and 200 microns.

X-ray diffraction (XRD) is an additional molecule- or phase-specific technique often used in research on historical paintings. XRD is an analytical technique that is used for the identification of crystalline components, such as original pigments employed by artists, but also newly formed chemical alteration products present within and at the surface of paint layers. When irradiating a sample with X-rays, the X-rays are scattered or diffracted by the component in specific directions. In XRD, the diffraction pattern of crystalline components in the analyzed location is collected, while amorphous components cannot be detected. Many of the mineralogical pigments have a defined XRD pattern, allowing for their straightforward identification. XRD also plays an important role in identifying degradation products in paintings, which are often crystalline. These degradation products cannot be identified with molecule-unspecific techniques, such as XRF. The probing depth of XRD is not very deep and most collected signals come from the first 10-50 micrometer below the surface of the painting.[36] In recent years, macroscale XRD scanners were developed to scan larger areas of paintings. MA-XRD scanners are not yet commercially available. The necessary scanning time per pixel is about 4 to 50 times longer in comparison to MA-XRF, limiting the size of the area that can be studied with this method.[37,30,36,28] The current spatial resolution of MA-XRD scanners is generally around 1 mm.

1.2.2 Microscale

Although the probing depths of the macroscale techniques vary from superficial (XRD, tens of μm) to all the way to the canvas (SWIR, IRR, MA-XRF hundreds of μm, depending on attenuation), with these methods it is difficult to trace back from what layer in the painting the collected signal is coming. As explained in section 1.1, the stratigraphy of oil paintings is complex and it is of great importance to know the buildup of the painting in order to understand how a painting was created, which chemical reactions are taking place, and what its current condition is. If non-invasive macroscale scanning did not answer all research questions, one or more small samples from the painting can be taken. The selection of sample locations is generally done based on non-invasive research using the methods described in the previous section. In this section, we will highlight the main microscale techniques used in heritage science research. A more complete overview can be found elsewhere.[38,39]

Generally, samples taken from oil paintings will be prepared as a cross section in a resin block, a method described by van Loon et al.[8] **Light microscopy** (LM) is usually the first technique that is used to investigate the paint cross section. A cross section is generally studied in reflected light. Different modes are used in LM: bright field, bright field with polarized light, dark field, and UV fluorescence. Visual information is obtained, and a trained microscopist is able to identify some of the materials in the sample. By using UV light to illuminate the sample, information on the varnish layer and some fluorescent components such as organic dyes can be obtained.[40] The resolution of light microscopy depends on the objectives used, but can be down to several hundreds of nanometers. **Polarized light microscopy** can be used to study crystalline material in thin sections.

Scanning electron microscopy (SEM) is another microscale technique often used to study paint cross sections at a very high resolution in 2D.[41,42] By using different detectors either the **secondary electrons** (SE) or the **backscattered electrons** (BSE) are measured. SE mode provides the best results when interested in studying the topography of the surface of the sample at a very high resolution. The greyscale of images collected in BSE mode can provide

some (limited) information on the chemical composition of the sample, as elements with a higher Z give a higher (whiter) contrast. In paint sample research, mainly BSE images are collected.[43] In combination with light microscopy, many standard paint components can be identified with SEM, especially with additional **energy-dispersive X-ray spectroscopy** (EDX) analysis to identify elements (equivalently to MA-XRF). The different layers in a paint stratigraphy can often be better distinguished with SEM in comparison to LM. Several degradation phenomena such as lead soap formation can also be studied with SEM.[41,44] The resolution of SEM depends on the used parameters such as voltage of the beam and spot size, but can be down to several nanometers.[39]

As in almost any chemistry research field, Fourier transformed **infrared spectroscopy** (FT-IR) is a much-used analytical technique in heritage science.[45–47] For embedded paint samples, specifically **micro attenuated total reflection**-Fourier transform infrared (ATR-FTIR) **imaging** is used. IR spectra are collected for a selected scan area. By selecting a ROI in the spectrum, micro-ATR-FTIR images can be produced that show the distribution of different functional groups of molecules in the sample. Micro ATR-FTIR can be used to study different aspects of paint samples, such as the pigment composition and organic components, but it is also a very valuable tool to detect the products of degradation phenomena such as surface crusts,[48] and metal soap protrusions.[49] The spatial resolution of ATR-FTIR imaging can be down to several micrometers.[39]

Raman spectroscopy is a powerful analytical technique for researching many different cultural heritage objects. Using micro-Raman spectroscopy, many pigments and some degradation products in paint cross sections can be identified. The oil medium, or other organic material present, can cause fluorescence, which complicates some identifications, especially those of very small particles in cross sections. Several pigments however are very strong Raman scatterers such as arsenic sulfides and vermilion (HgS). In the case of arsenic sulfides, a distinction can be made between the different arsenic sulfide such as orpiment and realgar, therefore being an important tool in identifying such species as SEM-EDX and ATR-FTIR cannot make these definitive distinctions. Raman spectroscopy uses laser probes as sources (usually varying from 488/514/532/633/785 nm). These can pose a risk to the samples, especially when the laser power is increased to get a better Raman signal, and one should be very careful when measuring as the sample can be damaged and then burn marks appear at the measured locations.[50,51] The resolution of micro-Raman spectroscopy is down to one or several micrometers.[39]

The identification of organic components and organic dyes in paint systems largely relies on techniques such as gas chromatography, mass spectrometry, and high performance liquid chromatography.[52] For the classic type of analysis of these techniques, small samples from the original material are needed. They cannot be performed on embedded paint samples and analysis is generally destructive. A technique that provides space-resolved organic (and inorganic) information in paint cross sections is **imaging secondary ion mass spectrometry** (SIMS).[53–55] It can be used to analyze the chemical composition of pigments and to image the presence of different elements in the paint, but based on the mass to charge ratio (m/z) also specific molecules can be imaged, e.g. palmitic acid in a smalt-containing paint.[53] Very high resolution results can be obtained, depending on the size of the beam which can be set to several hundred nanometers or several micrometers.[39]

Recently, **matrix assisted laser desorption ionization-mass spectrometry imaging** (MALDI-MSI) was performed on thin sections of embedded paint samples, operating at a spatial resolution of 10 µm.[56] Although the technique requires sampling and thus is invasive, the spatial information provides new insight into degradation processes of organic dyes and pigments, and the same area of the cross-section could first be studied using the other microscale techniques described in this chapter, before turning to MALDI-MSI. In biomedical imaging research, this imaging technique has already proven to be very promising.[57]

1.3 Synchrotron-based micro- and nanoscale techniques

The main drawbacks of the aforementioned lab-based techniques are that their detection limits are not always sufficient to detect all components. Especially degradation products that have formed in small amounts can be overlooked. Another challenge regarding lab-based techniques is to obtain a spatial resolution that is adequate for studying tiny paint samples of 50 - 500 µm – although this is not an issue for SEM. To overcome some of these issues, paint samples can be studied at a synchrotron light source, a specific type of particle accelerator.[58–62]

Theoretical background

Synchrotron light sources are extremely bright light sources that are used for scientific research. At a synchrotron radiation facility, a beam of electrons is generated by an electron gun (number (1) in **Figure 1.2**). This beam of electrons is accelerated by a LINAC (2) (linear accelerator) where, in a high vacuum environment, electromagnetic fields enable the acceleration of the beam to a speed that is close to the speed of light. The beam of electrons is then transferred into to the booster ring (3) where the energy of the electrons is increased, up to e.g. 3 GeV at SSRL (Stanford Synchrotron Radiation Lightsource, Menlo Park, USA)[63] or 6 GeV at PETRA III (DESY, Hamburg, Germany)[64] and ESRF (European Synchrotron Radiation Facility, Grenoble, France).[65] After being accelerated in the booster ring, the beam is directed into the storage ring (4). This storage ring has a very large circumference, differing in size from synchrotron to synchrotron. The circumference of the storage ring at ESRF is 844.4 meters, and that of PETRA III is even larger at 2.3 kilometer. In the storage ring, multiple bending magnets (5) guide the electron beam to follow the circular path. During the deflection of the beam due to the magnetic field, electromagnetic radiation is emitted. This electromagnetic radiation is what is commonly called synchrotron light. The light is emitted in the shape of a narrow cone and at a tangent from the circular path of the electrons. Special insertion devices (5) such as undulators and wigglers are placed in the straight sections of the storage ring. By forcing the beam onto a sinusoidal trajectory, these insertion devices stimulate the radiation and are responsible for the high spectral brightness of the beam.[66] The bright synchrotron light produced by these devices is directed to the beamlines (6) where the experiments take place. In the optics hutch of the beamline, a monochromator is used to separate the different wavelengths of the synchrotron light, and the desired wavelength for the experiment can be selected. Most synchrotrons have beamlines that use different parts of the electromagnetic spectrum, ranging from the IR to the X-ray region. In the optical hutch different X-ray optics, such as Kirkpatrick–Baez (KB) mirrors, are used to focus the beam. A smaller

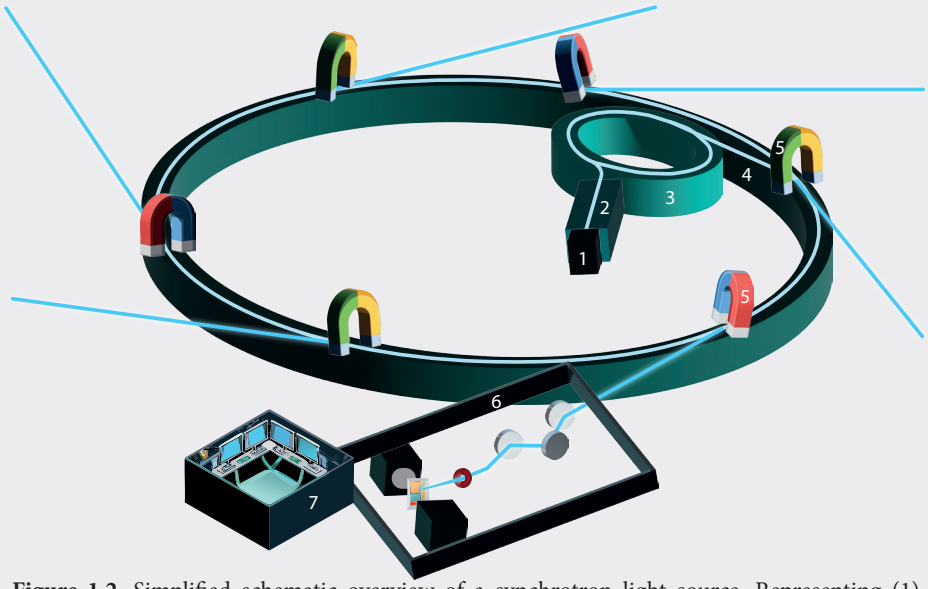

Figure 1.2. Simplified schematic overview of a synchrotron light source. Representing (1) electron gun, (2) LINAC, (3) booster ring, (4) storage ring, (5) bending magnets and insertion devices, (6) beam line, (7) control hutch.

beam size enables the researcher to scan their sample with smaller steps and therefore gives a higher resolution. The set-up and detectors present in the experimental hutch differ for every beamline and can be customized for the experiments that users want to perform. Scientist can follow their experiments from the control hutch (7). In general, an X-ray beamline is either a soft or hard X-ray beamline. There are no strict definitions of soft or hard X-rays, but generally the X-rays at a soft X-ray beamline have an energy between 100 and 3000 eV, whereas hard X-ray beamlines operate with X-rays at an energy between 3 to 100 keV. [67–70]

In summary, synchrotron light has several unique properties that make it an excellent light source for research.

- High spectral brightness: the number of photons emitted per second per bandwidth per unit solid angle and unit area of the source is extremely high.[66] The brightness is orders of magnitude higher compared to any lab sources, and even much higher than the light emitted by the sun.[71]
- High collimation: the beam has a small angular divergence.[69]
- Wide energy spectrum: synchrotron light covers a wide part of the electromagnetic spectrum, from infrared to X-rays, and an intense beam at any selected wavelength can be achieved. [69]
- Highly polarized: synchrotron light is highly polarized.[69]
- Short pulsed light emission: synchrotron light sources are excellent to perform time-resolved studies as it emits pulsed light, and the emitted pulses have a duration of less than a nano second. Due to the high spectral brightness the signal-to-noise ratio is typically very high and even short measurements provide high quality data.[69]

Theoretical background

X-ray fluorescence is based on the **photoelectric effect**.[75,76] When X-rays are bombarding the sample, different interactions can take place. Some X-rays will be transmitted, while others will be absorbed by the material. When the X-rays are absorbed, they can interact in different ways with the atoms in the sample. One of the interactions is scattering. When a photon interacts with the electrons of the atoms of a sample, two distinct types of scattering can take place: elastic and inelastic scattering. In elastic scattering there is no energy loss of the photons, this type is also called coherent or Rayleigh scattering. In inelastic scattering, also known as incoherent or Compton scattering, an energy loss occurs during the interaction, so photons emerge at a lower energy after this type of scattering took place.

Moreover, photons can interact with electrons in the core shells, a process referred to as photoelectric absorption. When the incoming photon has sufficient energy to remove one of the electrons from the core shell, a core electron can be excited to higher energy states or into the continuum, leaving a core hole. Due to this core hole the atom is in an excited state or ionized. The unstable excited or ionized atom then transitions to a more stable state through either Auger or fluorescent decay pathways. Auger decay involves the ejection of Auger electrons while electrons in the atom rearrange to restore the ground state. Alternatively, in fluorescent decay, the core hole is filled by an electron of higher energy, releasing the energy difference as an X-ray photon. The phenomenon is schematically shown in **Figure 1.3**. Auger and fluorescent decay processes compete and probabilities for each pathway also depend on the atomic element involved. Auger emission is predominant in lighter elements, while X-ray fluorescence is more prevalent in heavier elements. In the case of emission of an X-ray fluorescence photon, the energy of this photon is determined with a specialized detector, called an energy dispersive detector. The energy is a marker for the chemical element from which the photon has emerged. X-ray photons are collected over a certain energy range, resulting in an X-ray fluorescence spectrum. Based on this spectrum, the elemental composition of the sample can be determined.[77–80]

Synchrotron radiation based microscale X-ray fluorescence (SR-μ-XRF) is one of the techniques that can benefit paint sample research in comparison to lab based XRF analysis.[59,61,72–75] The main advantage of using synchrotron light for XRF is that the size of the beam can be tuned to a very small spot. In the studies reported in this thesis, we used a beam size of down to 200 by 300 nm at beamline P06 at PETRAIII (DESY, Hamburg, Germany). In this way, the resolution of an XRF map collected at the synchrotron will be much higher than any collected at a lab-based facility. Additionally, the high brilliance of the beam makes it possible to identify elements present at a very low concentration in the measured sample.

Synchrotron radiation-based microscale X-ray diffraction (SR-μ-XRD) has similar advantages as its fluorescence counterpart. As MA-XRD probes usually only the first 10-50 μm of the paint surface, a lot of additional information can be gained on the lower paint stratigraphy with SR-μ-XRD on a paint cross section. Scanning the samples with a very small beam can cause some issues: if the size of the beam is smaller than the size of the crystals in the sample, the resulting diffraction pattern is not a full representation of all the peaks expected, as not all crystal planes are probed. In some cases, this hampers successful identification and

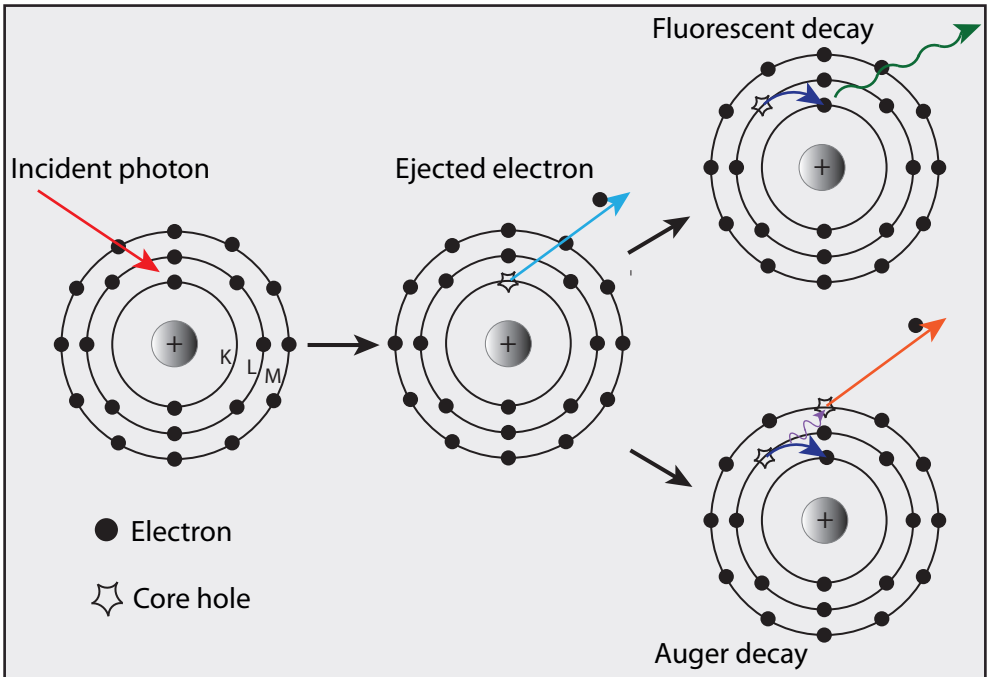

Figure 1.3. Schematic representation of the photoelectric effect. Two pathways can take place, fluorescent decay which results in the emittance of a characteristic X-ray, or Auger decay during which an Auger electron is emitted.

visualization of these components. Nonetheless, SR-μ-XRD has proven to be very valuable in elucidating degradation phenomena in paint samples. The degradation products often form in small crystals and therefore the aforementioned phenomenon is not an issue. SR-μ-XRD can be measured in both transmission and reflection geometry. [37,81–83] At some beamlines such as ID13 at ESRF and P06 at PETRA III, SR-μ-XRD and SR-μ-XRF can be performed simultaneously. The achieved spatial resolution depends on the beam line and available measuring time, but is typically in the range of 2 micrometer, but even down to 200 nm.

Theoretical background

X-ray diffraction (XRD) is a technique used to study the atomic and molecular structure of crystalline materials. When a crystal is irradiated with X-rays, the incident X-rays are scattered by the atoms in the crystal lattice. According to Bragg's law ($n\lambda = 2dsin\theta$), constructive interference occurs when the path difference between X-rays scattered by adjacent atomic planes, separated by an interplanar distance (d), equals an integer multiple (n) of the X-ray wavelength (λ). This interference produces a diffraction pattern characteristic of the crystal's atomic arrangement.

By analyzing the angles (θ) and intensities of the diffracted X-rays, the distances between atomic planes (d-spacings) and type and location of atoms within the crystal structure can be determined. XRD is widely used to identify crystalline phases, determine crystal orientations, and investigate lattice defects in materials.

X-ray absorption spectroscopy (XAS) is another technique that can identify specific molecules in paint samples.[58–60,84] XAS experiments are mainly conducted at synchrotron light sources, although there are examples of it being successful in the lab.[85] Mainly X-ray absorption near-edge spectroscopy (XANES) is used in the study of 17th century oil paint. A certain so-called X-ray absorption edge of an element of interest needs to be selected for a measurement. The change in the X-ray absorption coefficient is measured while tuning the energy of the incident beam across the characteristic energy of the element. Depending on the chemical state of the element, the absorption coefficient shows a characteristic modulation of its values, the so-called X-ray absorption fine structure (XAFS). In the case of arsenic sulfide pigments, for example, As-K edge XANES measuring the XAFS can easily distinguish As(III) from As(V) species, and it also shows a different spectrum for arsenic surrounded by oxygen species versus sulfur species.[86,87] As for SR-μ-XRF and -XRD, the resolution depends on the beam line but can be around 200 nm – 2 μm.

Theoretical background

X-ray absorption spectroscopy (XAS) is a technique used to study the electronic structure and local atomic environment of materials by analyzing how they absorb X-rays.[75,88–90] When X-rays of varying energy are directed at a sample, electrons can be ejected from core orbitals if the X-ray energy matches the binding energy of these electrons. The resulting absorption spectrum shows sharp features known as absorption edges, corresponding to specific core electron transitions. By examining the fine structure near these edges, known as XANES (**X-ray Absorption Near Edge Structure**) and EXAFS (Extended X-ray Absorption Fine Structure), detailed information about the oxidation state, coordination environment, and distances between atoms can be extracted.[89] XANES provides insights into the electronic state of the absorbing atom, while EXAFS informs on the distances, coordination numbers, and types of neighboring atoms. In general, the analysis of EXAFS data is more complex than that of XANES data, because XANES is often used as a fingerprint technique, comparing the XANES of unknown samples with spectra of known references. XAS data can be collected either in transmission mode or fluorescence mode, whereas fluorescence mode is often easier to use as it gives less sample restrictions. To obtain good data, the concentration of the studied element in the sample should not be too low (causing a poor signal-to-noise ratio), but also not too high as this can lead to self-absorption effects.[88]

XAS is (mostly) non-destructive and applicable to various states of matter, including solids, liquids, and gases. It is especially powerful in studying transition metals and complex materials where local atomic environments significantly affect their electronic properties.

1.4 Towards the third dimension

Two-dimensional microscale techniques have given a wealth of information on the stratigraphy and condition of paint samples. However, with the limited number of samples that can be harvested from a painting, it is important to get as much information as possible out of the samples available. Furthermore, two-dimensional information does not provide information on the 3D structure and morphology of the paint. Also to understand the size, shape and distribution of different components in the paint, two-dimensional techniques do not provide a full picture. To gain information in the third dimension, microscale tomographic methods can be used.[91] In this thesis, several tomographic microscale techniques are used to explore how they can be employed for the study of 17th century oil paints.

Theoretical background

Tomography is an imaging technique that reconstructs a 3D image of an object by combining multiple 2D projections taken at different angles.[92–95] The resolution of the reconstructed 3D volume is based on the resolution of the 2D images, the number of projections and the alignment between the images. The choice of the algorithm used for the 3D reconstruction also influences the accuracy and artifact suppression in the final image. Algorithms often used are filtered back projection or iterative methods like iART.[93] The iART (iterative Algebraic Reconstruction Technique) algorithm is used in tomography to iteratively refine image reconstructions from projection data. It starts with an initial guess of the object and compares calculated projections from this guess with the actual measured projections. Differences between the two are used to adjust the model of the object. This process is repeated iteratively, gradually improving the reconstruction until the calculated and measured projections closely match. iART is particularly effective for handling noisy or incomplete data (e.g. due to large angle steps) and is widely used in applications like medical imaging and materials science for accurate 3D reconstructions.[92–95] In this thesis, iART is used for the tomographic reconstructions. There is a loss of spatial resolution when going from 2D projections to a 3D reconstruction, depending on the number of projections collected and the quality of the collected data.

One of the first uses of tomographic techniques to study paint samples was **synchrotron-radiation based X-ray tomography**.[96,97] With this technique, a sample is scanned with X-rays of a certain energy, and the transmission of the X-rays is measured. This technique was used by Gervais et al. to look at the porosity in the ground of a 19th century painting.[98] Empty pores transmit more X-rays than the other material in the sample and the pores can therefore be separated by segmentation. Full field transmission X-ray microscopy (FF-TXM) was used by Liu et al. to study mass transport phenomena in model oil paint samples with a focus on the morphology and structure of the paint and porosity with a pixel size in 2D of several tens of nanometers.[99]

X-ray tomography does not provide any specific chemical information except the X-ray absorption. **Microscale X-ray diffraction tomography** is a very promising techniques as it could provide information on degradation phenomena taking place in paint samples in three dimensions. Several studies have used XRD tomography at the synchrotron to obtain a virtual cross section of a sample (beam size: 15 x 15 μm^2)[37] to study the degradation of red lead (pixel size: 4 x 5 μm^2)[100], and to unravel the lead and sulfur chemistry in a Rembrandt

paint sample (beam size: 2 x 2 μm^2).[101] The downside of this method is that to obtain a full 3D reconstruction of a sample instead of one or several virtual cross sections, the total scan time would be several days due to the needed dwell time per measured pixel to obtain good-quality XRD data.

Synchrotron-based microscale X-ray fluorescence tomography (SR-μ-XRF tomography) is more suited to scan paint samples, as a good signal-to-noise can be achieved in shorter measurement times. The first-time use of this technique on a historical paint sample is described in **Chapter 4** of this thesis. In other research fields, it has already been used in the last decades.[102] One of the areas of use is the study of heterogenous catalysts.[103,104] The spatial resolution can be down to several hundreds of nanometers.

Theoretical background

X-ray fluorescence tomography is a non-destructive imaging technique used to map the 3D distribution of elements within a sample.[75,94] The sample is irradiated by X-rays, and the characteristic emitted secondary (fluorescent) X-rays are detected to identify and (semi-)quantify element composition. The sample is rotated, and fluorescence data are collected from multiple angles. These projections are then used to reconstruct a 3D image of the element distribution. SR-based XRF tomography is highly sensitive to trace elements and provides spatial resolution at the micro to nanoscale when executed at synchrotron micro- or nanoprobe beamlines. XRF tomography faces some difficulties due to matrix effects, which causes re-absorption of emitted photons on their way out of the sample, and can cause the element distribution, especially of lighter elements, to be somewhat inaccurate.[102] Due to these artifacts, X-ray fluorescence tomography is mainly suited to be used in a qualitative or semi-quantitative way, and full quantitative concentration calculations are not possible.

Ptychography is a coherent imaging method that can be used to visualize the difference in electron density within a sample. Ptychographic tomography provides a 3D visualization of a sample. Ptychographic X-ray computed tomography was used to study the morphology and composition of microfossils.[105] Several studies show the successful combination of SR-μ-XRF tomography and ptychographic tomography.[106–108] The additional value of ptychography in the case of paint sample research is the ability to image low Z elements, simultaneously with high electron density components. Correlated SR-μ-XRF and ptychographic tomography was used in **Chapter 4** to study the ground and preparatory layers of *The Night Watch*. Ptychography can reach a resolution of a few nanometers.[109]

Theoretical background

X-ray ptychography is an advanced imaging technique that uses coherent X-rays to generate high-resolution phase-contrast images of a sample. Unlike traditional X-ray imaging, which captures intensity variations, ptychography relies on interference patterns (diffraction patterns) produced as X-rays pass through or are scattered by a sample. The technique involves scanning the sample in overlapping regions with a focused X-ray beam, where each position produces a unique diffraction pattern. These diffraction patterns contain information not only about the intensity of the scattered X-rays but also about the phase shifts that occur as the X-rays interact with the sample's internal structure. This phase information is crucial because it reveals fine details about the sample's internal composition and structure that are not visible through intensity

alone. By combining data from multiple overlapping regions, an iterative algorithm reconstructs a high-resolution image of the sample, often surpassing the resolution limits of conventional X-ray microscopy relying on focusing optics such as mirrors. Ptychography is particularly advantageous for imaging samples with complex internal structures. Since ptychography can achieve resolutions down to the single nanometer scale, it is used for investigating materials at levels close to the atomic and molecular regimes. Additionally, it is (typically) non-destructive, making it suitable for delicate samples. The technique can be performed in both two and three dimensions, providing volumetric information about the sample. Synchrotron light sources are used for X-ray ptychography because they provide the necessary coherent and intense X-ray beams.[110–112,109,113]

1.5 Smalt, arsenic and lead-based pigments and their degradation

The number of materials used as pigments in the 17th century paintings is extensive and ranges from minerals found in nature such as iron-containing earth pigments to manufactured pigments such as lead white and blue verditer. We will not discuss all available pigments here, as good overviews can be found in many other sources.[38,40,114–117] Instead, we will focus on the pigments appearing in this thesis. The changing appearance of oil paintings over the centuries, as mentioned before, is partly due to the degradation of the pigments used in the painting. A wide range of chemical processes can occur, resulting in damage that manifests in different forms, such as discoloration, formation of new materials and flaking of paint. One pigment can undergo different types of degradation and through different degradation pathways. This depends on the local environment of the pigment. Factors that contribute to this are: the local alkaline/acidic conditions, exposure to light, exposure to gasses and interaction with other materials such as pigments, fatty acids and other organic materials.[3,118] Accurate prediction of paint degradation is challenging because from a chemical perspective, paints are very heterogenous with a combination of inorganic and organic materials. This heterogeneity allows for many chemical reactions, rendering paints highly complex materials.

For the materials relevant in this thesis, we will briefly describe their characteristic properties as well as related degradation processes.

1.5.1 Arsenic sulfide pigments

Orpiment (As_2S_3) is a yellow arsenic sulfide pigment that have been used as pigment since antiquity. It is a monoclinic mineral with a crystal structure made of sheets. Orpiment was also sold under other names such as 'king's yellow', *Rauschgelb* and *jaune royal*.[119] Throughout its history, it has been used for many different objects, from Egyptian tombs to medieval manuscripts.[119–121] In 17th century oil paintings, it was used in many still-life paintings for the painting of yellow flowers and lemons.[122,123] The name orpiment originates from the Latin name *auripigmentum*, literally meaning 'gold paint'.

Realgar (α-As_4S_4) is an arsenic sulfide mineral known for its distinctive red-orange color. The monoclinic mineral consists of single molecules connected by Van der Waals forces. It is often found together with orpiment in mines. Realgar has been found in ancient Egyptian make

up, as medicine in ancient Greece, and in sixteenth century Bulgarian icons.[119] Although it is often mentioned as pigment for oil paint, it is rarely confirmed by analytical techniques.[119,120]

In addition to the natural minerals, many **synthetic arsenic sulfide pigments** were made as early as the fifteenth century.[121,124] One of these is the synthetic 'artificial orpiment', which was produced from the 16th century.[124] Artificial orpiment has been found in the oeuvre of Rembrandt.[125] Amorphous arsenic sulfide glasses were also used as pigments, in a wide variety of hues, depending on their arsenic and sulfur ratios.[126] It is debatable to what extent the artists of the 17th century knew exactly with what material they were painting.[121]

Degradation

Orpiment is known to be a light sensitive pigment. Irradiation with light can induce the formation of arsenolite (As_2O_3), which has a pale yellow to white color. Next to arsenolite, studies showed that also arsenate (As^{5+}) species are present in oil paintings and other art objects containing arsenic sulfides.[86,87,127] For some time the hypothesis was that these arsenate species were derived from the arsenolite formed during light exposure. However, in this thesis in **Chapter 2**, we present a second mechanism for the degradation of orpiment not including the formation of arsenolite. In this second reaction mechanism, not the exposure to light but the exposure to a medium is crucial.

The formed arsenates species can further react into secondary degradation products, namely metal arsenates. These metal arsenates originate from the arsenates ($H_3AsO_{4(aq)}$, $H_2AsO_4^-{}_{(aq)}$, $HAsO_4^{2-}{}_{(aq)}$, or $AsO_4^{3-}{}_{(aq)}$) that react with available metal ions. In literature, mainly lead arsenates are described to have formed in oil paintings. So far, two lead arsenates have been identified in paintings: schultenite ($PbAsO_4$) and mimetite ($Pb_5(AsO_4)_3Cl$).[36,86,123,128,129] Also in **Chapter 2** and **3** of this thesis, these degradation products were found and described. Aside from lead arsenates, arsenates with different metals can form. Calcium arsenates and iron arsenates are the most probable to form in paintings. The species were found in manuscript and wall paintings, and an indication of a calcium arsenate was found in an oil painting by Coorte.[86]

The yellow pararealgar (β-As_4S_4) is a light induced degradation product of the red mineral realgar. For a long time, it was often misidentified as orpiment when a yellow component containing arsenic and sulfur was found. The first description of pararealgar was made in 1980 by Roberts et al.,[130] but it was not until 1996 that pararealgar was fully described and identified as a separate component.[131] During the formation of pararealgar, it is possible that arsenolite is formed from realgar. Exposure of pararealgar to light can also further stimulate the formation of arsenolite.

1.5.2 Lead-containing materials

Another heavy metal often encountered in 17th century paintings is lead. Lead can be present both in various pigments and in the binder of paint. In **Chapter 4** the discovery of an unexpected lead-containing layer in *The Night Watch* is described, partly explaining its current condition, in which many lead soap protrusions are present.
Some of the relevant lead containing components are described here.

Lead white usually consists of a mixture of **cerussite** (lead carbonate, $PbCO_3$) and **hydrocerussite** (basic lead carbonate, $Pb_3(CO_3)_2(OH)_2$). It was the most used white pigment in the 17th century, due to its high hiding power in comparison to materials such as chalk

(calcite, $CaCO_3$) and gypsum ($CaSO_4 \cdot 2H_2O$). Lead white is not a naturally occurring product but was manufactured by mankind as early as 300 B.C., making it one of the oldest synthetically produced pigments.[115,132,133] Different methods were used, but generally the 'old Dutch method' or 'stack process' can be considered as the standard production method for lead white encountered in 17th century Netherlandish oil paintings. In this procedure, sheets of metallic lead (Pb) are rolled up and exposed to vapors of vinegar (acetic acid, CH_3COOH). This is put into earthenware pots, which are covered by a pile of horse manure inside a shed (providing heat and CO_2). After some time, lead white is formed on the surface of the metallic sheets of lead and the white flakes are scraped off to obtain the pigment.[134–136] From the metallic lead, lead acetates are formed first which are then converted into hydrocerussite through the intermediate plumbonacrite ($Pb_5(CO_3)_3O(OH)_2$), which is a rare lead carbonate. Hydrocerussite reacts with CO_2 to form cerussite, and the longer the process is left taking place, the more cerussite is formed. The ratio between hydrocerussite and cerussite can therefore be different in different batches of lead white.[136,137]

Red lead or **minium** (Pb_3O_4, $Pb^{2+}_2Pb^{4+}O_4$) is another lead-containing pigment. This red to orange pigment can both be found in nature or it can be synthetically produced by heating hydrocerussite or lead(II)oxide in air. Most red lead pigment sold in the 17th century was artificially produced, by roasting hydrocerussite or litharge.[133]

Litharge (α-PbO, tetragonal, red) and **massicot** (β-PbO, orthorhombic, yellow) are two lead-containing materials that can also be found in paintings. By heating litharge, the high temperature polymorph massicot can be formed. Litharge was often added to the oil binder to speed up the drying of the oil.[133,137] Although the mineral litharge is lead(II) oxide in tetragonal lattice structure, in historical painters' literature, the term *litharge* is actually often used to refer to lead(II) oxide in orthorhombic lattice structure (massicot). The drier effect is twofold, the lead ions accelerate the uptake of oxygen and autoxidation of the oil and lead also accelerates the polymerization of the oil into a firm film. The use of litharge as red pigment is not common.[16,138] Massicot was more often used as pigment for its yellow color.

Degradation

The degradation of lead components is a complex topic as it covers a wide range of reactions and different end products. One of the most studied degradation phenomena related to lead is the formation of lead soaps.[6,139,140] Lead soaps are a phenomenon first identified and described in historic oil paintings at the end of the 20th and beginning of the 21st century.[141,142] In the formation of lead soaps, lead ions (Pb^{2+}) react with free fatty acids deriving from the TAGs of the drying oil into lead ionomers. These ionomers can aggregate to become lead soaps.[14,143] Due to their low solubility in oil, these lead soaps can crystallize and become so-called lead protrusions. Lead protrusions are small white globules, which can form within the paint layers, but they can also disrupt the top layer of the painting and become visible at the paint surface. The small white 'spots' can have a disrupting effect for the viewer of a painting, especially if they form within dark areas or in finely painted areas such as faces in a painting. These lead protrusions sometimes become disconnected from the underlying layers and they can physically fall out of the painting, leaving a small hole in the (top) paint layers of a painting. [44,141,144]

Next to the formation of the lead soaps, lead ions can also form secondary degradation products with other components available in the paint layers. In the arsenic sulfide section, we already discussed the formation of lead arsenates when lead ions (Pb^{2+}) react with arsenates.

In various paintings, lead sulphates have been identified. Two different lead sulphates have been found so far in 17th century oil paintings: anglesite ($PbSO_4$) and palmierite ($K_2Pb(SO_4)_2$). It is often difficult to identify the source of all elements in degradation products. In this case, the sulfur present in both degradation products may originate from sulfur in the surrounding atmosphere. Especially in the past ages, the content of SO_2 in the air was high due to the open fires to heat up rooms and due to air pollution from industry. Another probable source for the sulfur are materials in the painting such as vermillion (HgS) or alum, used as red lake substrate (generally $AlK(SO_4)_2 \cdot 12H_2O$).[36,128,145–147] The potassium found in palmierite can originate from different materials in the paint, for example from degraded smalt or from alum.[128,145,146]

Another lead-containing secondary degradation product that has recently been found is lead formate ($Pb(HCOO)_2$).[148] These type of studies show that state-of-the-art analytical techniques enable researchers to find degradation products that are present in low concentrations that were so far undiscovered.

Lead white and red lead are incompatible with orpiment, due to the risk of the formation of galena (PbS).[149] A second form of discoloration of red lead can take place, i.e. a whitening instead of a darkening. In this case, the red lead (Pb_3O_4) transforms either into lead sulfate (anglesite) or into lead carbonates (cerussite and hydrocerussite). During the formation of these lead carbonates, again plumbonacrite is formed as intermediate product.[100]

Plumbonacrite was also found in the impasto paint layers of Rembrandt van Rijn. In this case, the most probable hypothesis is that Rembrandt used an (alkaline) litharge-treated oil for the impastos, to influence the rheological properties of the paint. In view of its alkaline properties, the litharge (PbO) may have undergone a carbonation reaction during which plumbonacrite was formed. Alternatively, the alkaline local conditions resulting from the presence of the litharge oil may have caused (hydro)cerussite to transform to plumbonacrite *in-situ*.[137]

1.5.3 Smalt production and degradation

Smalt is a man-made blue pigment that consists of ground potash glass colored by the addition of cobalt. Different minerals were used throughout history as the source of cobalt. The main mineral since the Middle Ages was smaltite $[Co,Ni]As_{3-2}$, and from the 16th and 17th century onwards the minerals erythrite ($[Co,Ni]_3[As\ O_4]_2 \cdot 8H_2O$) and cobaltite (Co,Fe)AsS were used as well.[150–152] The initial step of smalt production involved the selection and purification of cobalt ores to obtain high-quality cobalt oxide. The ores were roasted, washed, grinded and then separated by levigation to eliminate some of the impurities such as arsenic, sulfur and copper. These impurities could influence the purity and intensity of the color. The residue was mixed with some sand or quartz to obtain a mixture named *zaffre*. [153,154] The *zaffre* was then mixed with silica and potash (potassium carbonate). Potash acts as a flux and decreases the needed temperature to melt the mixture.[155,156] The mixture was then heated in a glass oven or kiln to fuse the ingredients together. This mixture was cooled by pouring it into cold water, and solid blue glass mass was obtained. This mass was crushed into fine particles to obtain the pigment smalt. The smalt was ground into different particle sizes, directly effecting the color hue of the pigment. Fine particles give a more greyish smalt, while larger particles result in a more blue pigment.[115,152]

Degradation

In **Chapter 5**, we study the composition and degradation of different smalt-containing paint mixtures used by Rembrandt van Rijn in *The Night Watch*. The discoloration of smalt can cause blue or purple paint to become translucent or a greyish brown.[157,158] Potassium ions (K^+) have been shown to leach from smalt particles.[53,159,160] These potassium ions act as charge compensator to stabilize the tetrahedral coordination of the cobalt ions. When the potassium ions have leached from the structure, the coordination of the cobalt ions changes to octahedral coordination. In this process, the Co-O bonds are elongated and the number of neighboring oxygen atoms to the cobalt ions increases. This change in the ligand field around the cobalt ion results in the loss of the blue color. The change from intense blue to colorless is directly related to the alkali ion content, in the case of smalt, the potassium

1.6 Operation Night Watch

The research of **Chapters 3**, **4** and **5** are part of the research phase of *Operation Night Watch*, taking place at the Rijksmuseum from 2019 onwards. An introduction to the painting and the project is given here.

1.6.1 *The Night Watch*

The painting *Officers and other civic guardsmen of District II in Amsterdam, under the command of Captain Frans Banninck Cocq and Lieutenant Willem van Ruytenburch* (1642) by Rembrandt van Rijn is the centerpiece of the Rijksmuseum in Amsterdam (see **Figure 1.4**). The painting is more commonly known as *The Night Watch*, a nickname given to the painting at the end of the 18th century. The civic guards' portrait was made on commission for the Great Hall of the *Kloveniersdoelen*, the headquarters of the arquebusiers' civic guards.[162,163]

While other civic guards' portraits from the 17th century were often rather static, showing the guards posing with their weaponry and attributes in standing position, or guards sitting around a table during a festive meal, by contrast, the scene in *The Night Watch* is a lot more dynamic. The observer feels as an eyewitness of the depicted moment in time, when the guardsmen are starting to march. The dog on the right is startled by a loud bang on the drum, the musketeer in red is preparing his musket with gunpowder, and Captain Frans Banninck Cocq's hand gesture invites the men to start their march. Rembrandt's use of light and shadow (*chiaroscuro*) increases the dynamic character and the dramatic effect of the scene.

In the more than 380 years long lifespan of the oil painting, it has been subjected to at least 31 restoration treatments, several changes of location and a few physical attacks. A complete overview of the treatment history can be found elsewhere,[164–166] yet, some of the more impactful moments in the object's history will be highlighted here.

In the Rijksmuseum, *The Night Watch* plays a key role as Rembrandt's *magnum opus* but is also considered to be the most important painting in the Netherlands.

Around 1715, the painting was moved from the Kloveniersdoelen to a new location: the *Kleine Krijgsraadkamer* (Small War Council Room) of the Amsterdam Town Hall. *The Night Watch* did not fit on the designated wall of the room, and therefore strips of canvas were removed from all four sides of the painting.[164] Especially on the left side of the painting a large strip was removed, eliminating two figures. The contemporary copy attributed to Gerrit Lundens (ca.

Figure 1.4. *The Night Watch* by Rembrandt van Rijn (1642, Rijksmuseum Amsterdam, oil on canvas, 410 cm by 485 cm).

1642-1655, National Gallery of London), shows what is presumed to be the entire original composition.[163] In 1815, *The Night Watch* was moved to the *Trippenhuis* in Amsterdam until it was placed in the specially designed *Night Watch Room*, at the end of the *Gallery of Honour* at the heart of the new building of the Rijksmuseum in 1885. During the Second World War, the painting was evacuated from the museum for safe keeping. From September 1939, it was placed in four different bomb shelters: the Radboud castle in Medemblik, a shelter in Castricum, a shelter in Heemskerk and from 1942 onwards in the 'safe' (*kluis*) in the limestone caves of the Sint Pietersberg in Maastricht. For the shelter in Castricum, the painting was rolled on a cylinder, on which it remained until the end of World War II.[164] After its return to the museum in Amsterdam in June 1945, an elaborate restoration campaign was executed which lasted for two years.[164,165]

On 14 September 1975 a mentally disturbed[167] man attacked *The Night Watch* with a serrated table knife. Despite the quick intervention of a guard and a bystander, the man managed to make 12 cuts in the painting.[164] To repair the significant damage to the painting, a large restoration project was needed. Next to the mending of the tears, a wax-resin lining treatment and removal and reapplication of the varnish were also executed. In two moments during the treatment, scientists from the Central Research Laboratory for Objects of Art and Science (Amsterdam) were involved to perform analysis on the painting.[168–170] The savage cuts in the

painting had caused the splintering of paint and the loss of many small paint fragments, many of which were collected by the researchers from the frame and from the floor two days after the attack. One of these samples has played a special role in **Chapter 4**, where it turned out to be the missing puzzle piece in the discovery of an unknown technique used by Rembrandt.

In 1990, *The Night Watch* was again the victim of violence. This time, a man attacked the painting with a spray can containing sulfuric acid. A guard on duty acted quickly by apprehending the man, while a second guard started spraying water over the affected area, limiting the damage inflicted by the acid. Eventually only in the areas directly affected by the acid, the varnish needed to be replaced.[164]

1.6.2 Operation Night Watch

Some 45 years after the last extensive treatment of *The Night Watch* in 1975-76, there were new concerns about its condition. Some deformations were visible in the upper right area of the painting, dark areas of the painting had become difficult to 'read' due to increased darkening of the varnish, and whitish crusts were visible at the surface of the painting. These concerns, together with the fast innovation and development of analytical techniques in the field of heritage science, led to the initiation of *Operation Night Watch* at the Rijksmuseum.[171] In July of 2019, the research phase (phase 1) of *Operation Night Watch* started. The multi-year project was developed around three main research questions:

- How did Rembrandt create *The Night Watch*?
- What is the current condition of *The Night Watch*?
- What is the best way to ensure its long-term preservation?

A specially designed glass enclosure was built around the painting (see **Figure 1.5**) so that most of the research could take place in public view. The large team of *Operation Night Watch* includes chemists, physicists, data scientists, conservators and art historians. Many of the techniques were employed in collaboration with museums, universities and private companies from the Netherlands and abroad.

The project started with MA-XRF scans of the entire painting. The painting was hung on an easel that allowed it to be moved in the X, Y and Z directions. Two large scissor lifts were placed on rails in front of the painting, and in this way all corners of the large painting could be reached by equipment placed on the lifts. Daylight photography (normal, raking and transmitted light), infrared photography (reflected and transmitted), UV light photography and X-ray photography of the complete painting were executed. A stereomicroscope was mounted on the scissor lifts to study many areas of the painting, using normal and UV light. Selected areas were studied using optical coherence tomography (OCT) in collaboration with the Amsterdam University Medical Center. In collaboration with the University of Antwerp, MA-XRPD mapping was performed on a selection of areas of the painting.

In addition, a specially designed imaging frame was installed in front of the painting. Several cameras and instruments could be placed on this frame to scan the painting more easily. This frame was used for the high resolution (20 and 5 micrometer resolution) day light photography[172] and for the reflectance imaging spectroscopy examinations.[31] RIS was performed in collaboration with the National Gallery of Art, Washington DC. 3D photography and shearography studies of the painting were performed in collaboration with Delft University of Technology. Some selected areas were additionally studied with Hirox

Figure 1.5. Picture taken in *The Gallery of Honour* in July 2019 at the start of *Operation Night Watch*. A glass enclosure was built around the painting. Non-invasive imaging measurement on the macroscale were performed in front of the public, as well as stereomicroscopic research and sampling of the painting. Image by Rijksmuseum.

3D microscopy. Cleaning tests were performed using laser speckle imaging, through a collaboration with Wageningen University & Research and NanoMoi. Fiber optical reflectance spectroscopy and reflected Fourier-transformed infrared spectroscopy measurements were performed on several locations of the painting.

After the first period of the research phase, the structural treatment of the painting was started (phase 2). As the canvas was sagging in some parts of the painting, it was removed from its wooden stretcher and a new stretcher was made. This stretcher comprises adjustable springs, which make it easier to correct for changes in the canvas over time. This system was designed by Antonio Iaccarino Idelson. Vibration measurements and digital modeling of the behavior of the painting were performed by Kerstin Kracht.

Alongside the research taking place in the glass enclosure at the Gallery of Honour, a substantial volume of research was done at the *Ateliergebouw*, the building where the Rijksmuseum's conservation studios and research labs are located, and at external research facilities. At the *Ateliergebouw*, the many paint samples taken during the research phase were carefully embedded in either Technovit® 2000 LC or Poly-Pol resin. Before and after embedding, the samples were studied using light microscopy (bright field, dark field, UV). Many samples were studied using micro-ATR-FTIR imaging in collaboration with the University of Amsterdam and the Cultural Heritage Agency of the Netherlands. The latter also performed high resolution liquid chromatography and mass spectroscopy, and photodiode array detection measurements on tiny scrapings from the painting. Pyrolysis and headspace gas chromatography coupled with mass spectrometry were performed in collaboration between

the Rijksmuseum and the Cultural Heritage Agency of the Netherlands. At the Rijksmuseum, some of the samples were studied using Raman spectroscopy. Almost all samples were studied using SEM-EDX. Around twenty samples were brought to synchrotron facilities (Deutsches Elektronen-Synchrotron (DESY, Hamburg), the European Synchrotron Radiation Facility (ESRF), Grenoble) for measurements involving SR-µ-XRD, SR-µ-XRF, or tomographic SR-µ-XRF correlated with ptychography.

Rheological studies on paint reconstructions were performed in collaboration with AkzoNobel. Lead-isotope analysis was performed on samples from *The Night Watch* by the Vrije Universiteit Amsterdam. At the Eindhoven University of Technology finite element modeling and micro tensile testing of fibers was performed. Differential scanning calorimetry and melting point analysis was performed in collaboration with the University of Amsterdam.

Phase 3 of *Operation Night Watch* started in November 2024. During this phase the varnish layers and old overpaint will be removed from the painting. This phase will again take place in front of the public, in a slightly adjusted setting compared to the situation shown in **Figure 1.5**. In this phase the gained research results from the research phase (phase 1) will be consulted as well as new measurements will be carried out to support and monitor the cleaning process and to support decision making. The measurements consist of non-destructive analytical techniques, like laser speckle imaging and reflectance FTIR on the painting, and analyses of cleaning materials with headspace and pyrolysis GC-MS, LM and SEM. Phase 3 will be followed by the application of fillings, retouches and varnishing (phase 4). In phase 5, *The Night Watch* will be placed in a new frame. Following the completion of the treatment, the condition of the painting will be monitored on the long term to ensure its preservation and presentation for future generations.

1.7 Scope of this thesis

The overall goal of this thesis is to explore what advanced synchrotron-based imaging methods, and specifically three-dimensional methods, can add to the knowledge of 17th century paint and degradation phenomena taking place in these oil paint systems.

In **Chapter 2**, the degradation pathways of orpiment (As_2S_3) are studied. Next to the formation of arsenolite (As_2O_3), As(V) species are found as degradation products using synchrotron based XANES. In this chapter we study how different local conditions (light versus dark, dry versus in a medium) influence the degradation pathway of orpiment in paint systems. The light induced degradation pathway was additionally studied using tomographic full field X-ray transmission microscopy (TXM). By repeating TXM scans at different energies, both the physical as well as the chemical changes caused by light induced ageing could be studied. The results observed in the simple model systems are compared to a case study of a paint sample from a 17th century still-life painting of Jan Davidsz, De Heem.

Chapter 3 investigates the use of arsenic sulfide pigments in *The Night Watch*. Arsenic sulfide pigments were only found in the sleeves and in the embroidery of the costume of Lieutenant Willem Ruytenburch, one of the key figures of the painting. Rembrandt used arsenic sulfide pigments to mimic gold threads in this buff coat. By using Raman spectroscopy, the exact types of (unexpected) arsenic sulfides were determined, and SR-µ-XRD measurements provided insight in the degradation phenomena taking place in the painting. Secondary formed degradation products were found that show that degradation products of the arsenic

sulfides have reacted with other paint components. The discovery of the arsenic sulfide pigments, which were not found in other paintings of Rembrandt so far, are contextualized with an extensive study of historical sources.

In **Chapter 4** the first-time study of an historical paint sample using correlated ptychographic and X-ray fluorescence nano-tomography is presented. It is also, to our knowledge, the first-time use of the two separate three-dimensional imaging techniques on a paint sample. For this study, a paint sample of the ground layer of Rembrandt's *The Night Watch* was brought to beamline P06 at PETRA III (DESY, Hamburg). The tomographic XRF data provides information on the composition of the ground. The extra dimension provides more insight in the shape of pigment particles and the relation between components compared to two-dimensional imaging methods such as SEM-EDX. Low Z element components could be visualized using the ptychographic data. A – so far unknown – special preparatory layer of the canvas was revealed with this study, which was confirmed with macroscale measurements on the painting as well as by an historical source.

In **Chapter 5** X-ray fluorescence tomography is used to study the different paint mixtures containing smalt in *The Night Watch*. By studying three samples originating from different areas of the painting, the smalt used with different purposes could be compared. The particle size of the smalt particles was quantified. The XRF data was used to determine the chemical fingerprint of the smalt particles, clustering the particles based on the differences in composition. By using the volume percentages of the different components, the composition of the smalt paint mixtures, containing also other pigments such as azurite (a blue copper-based pigment, $Cu_3(CO_3)_2(OH)_2$), was quantitatively estimated. The results are used to study whether one or multiple types of smalt were used in *The Night Watch*.

In **Chapter 6**, a conclusion of the work is given, together with future perspectives related to microscale paint research gained through this work. This is followed by an overview of the publications, presentations and outreach based on this work and a summary of the work in both English and Dutch.

1.8 References

(1) Ankersmit, B.; Stappers, M. H. L. *Managing Indoor Climate Risks in Museums*; Cultural Heritage Science; Springer International Publishing, 2018.

(2) *Managing Collection Environments: Technical Notes and Guidance*; Taylor, J. T., Beltran, V. L., Eds.; Getty Conservation Institute: Los Angeles, CA, 2023.

(3) Miliani, C.; Monico, L.; Melo, M. J.; Fantacci, S.; Angelin, E. M.; Romani, A.; Janssens, K. Photochemistry of Artists' Dyes and Pigments: Towards Better Understanding and Prevention of Colour Change in Works of Art. *Angewandte Chemie - International Edition* **2018**, *57* (25), 7324–7334. https://doi.org/10.1002/anie.201802801.

(4) Keck, S. Mechanical Alteration of the Paint Film. *Studies in Conservation* **1969**, *14* (1), 9–30. https://doi.org/10.1179/sic.1969.002.

(5) Pouyet, E.; Cotte, M.; Fayard, B.; Salomé, M.; Meirer, F.; Mehta, A.; Uffelman, E. S.; Hull, A.; Vanmeert, F.; Kieffer, J.; Burghammer, M.; Janssens, K.; Sette, F.; Mass, J. 2D X-Ray and FTIR Micro-Analysis of the Degradation of Cadmium Yellow Pigment in Paintings of Henri Matisse. *Applied Physics A: Materials Science and Processing* **2015**, *121* (3), 967–980. https://doi.org/10.1007/s00339-015-9239-4.

(6) *Metal Soaps in Art: Conservation and Research*; Casadio, F., Keune, K., Noble, P., Van Loon, A., Hendriks, E., Centeno, S. A., Osmond, G., Eds.; Cultural Heritage Science; Springer

International Publishing: Cham, 2019. https://doi.org/10.1007/978-3-319-90617-1.
(7) *Conservation of Easel Paintings*, 2nd ed.; Stoner, J. H., Rushfield, R., Eds.; Routledge: London, 2020.
(8) van Loon, A.; Keune, K.; Boon, J. J. Improving the Surface Quality of Paint Cross-Sections for Imaging Analytical Studies with Specular Reflection FTIR and Static-SIMS. In *art'05 - 8th International Conference on "Non Destructive Investigations and Micronalysis for the Diagnostics and Conservation of the Cultural and Environmental Heritage."*; Lecce (Italy), 2005.
(9) Walter, P.; De Viguerie, L. Materials Science Challenges in Paintings. *Nat. Mater.* **2018**, *17* (2), 106–109. https://doi.org/10.1038/nmat5070.
(10) Ranquet, O.; Duce, C.; Bramanti, E.; Dietemann, P.; Bonaduce, I.; Willenbacher, N. A Holistic View on the Role of Egg Yolk in Old Masters' Oil Paints. *Nat Commun* **2023**, *14* (1), 1534. https://doi.org/10.1038/s41467-023-36859-5.
(11) Bonaduce, I.; Duce, C.; Lluveras-Tenorio, A.; Lee, J.; Ormsby, B.; Burnstock, A.; Van Den Berg, K. J. Conservation Issues of Modern Oil Paintings: A Molecular Model on Paint Curing. *Acc. Chem. Res.* **2019**, *52* (12), 3397–3406. https://doi.org/10.1021/acs.accounts.9b00296.
(12) Hermans, J. J.; Keune, K.; Van Loon, A.; Corkery, R. W.; Iedema, P. D. Ionomer-like Structure in Mature Oil Paint Binding Media. *RSC Adv.* **2016**, *6* (96), 93363–93369. https://doi.org/10.1039/C6RA18267D.
(13) Orlova, Y.; Harmon, R. E.; Broadbelt, L. J.; Iedema, P. D. Review of the Kinetics and Simulations of Linseed Oil Autoxidation. *Progress in Organic Coatings* **2021**, *151*, 106041. https://doi.org/10.1016/j.porgcoat.2020.106041.
(14) Hermans, J. J.; Van Loon, A.; Keune, K.; Iedema, P. D. Toward a Complete Molecular Model for the Formation of Metal Soaps in Oil Paints. In *Metal Soaps in Art: Conservation and Research*; Casadio, F., Keune, K., Noble, P., Van Loon, A., Hendriks, E., Centeno, S. A., Osmond, G., Eds.; Cultural Heritage Science; Springer International Publishing: Cham, 2019. https://doi.org/10.1007/978-3-319-90617-1.
(15) DePolo, G.; Iedema, P.; Shull, K.; Hermans, J. Comprehensive Characterization of Drying Oil Oxidation and Polymerization Using Time-Resolved Infrared Spectroscopy. *Macromolecules* **2024**, acs.macromol.4c01164. https://doi.org/10.1021/acs.macromol.4c01164.
(16) Tumosa, C. S.; Mecklenburg, M. F. The Influence of Lead Ions on the Drying of Oils. *Studies in Conservation* **2005**, *50* (sup1), 39–47. https://doi.org/10.1179/sic.2005.50.Supplement-1.39.
(17) Baij, L.; Chassouant, L.; Hermans, J. J.; Keune, K.; Iedema, P. D. The Concentration and Origins of Carboxylic Acid Groups in Oil Paint. *RSC Advances* **2019**, *9* (61), 35559–35564. https://doi.org/10.1039/c9ra06776k.
(18) Nardelli, F.; Martini, F.; Lee, J.; Lluvears-Tenorio, A.; La Nasa, J.; Duce, C.; Ormsby, B.; Geppi, M.; Bonaduce, I. The Stability of Paintings and the Molecular Structure of the Oil Paint Polymeric Network. *Sci Rep* **2021**, *11* (1), 14202. https://doi.org/10.1038/s41598-021-93268-8.
(19) Noble, P.; Verslype, I. The Use of X-Radiographs in the Study of Paintings. In *Counting Vermeer : using weave maps to study Vermeer's canvases*; Franken, M., Wheelock, A. K., Johnson, C. R., Sethares, W. A., Eds.; RKD (Rijksbureau voor Kunsthistorische Documentatie), Netherlands Institute for Art History: The Hague, Netherlands, 2017.
(20) Asperen de Boer, J. R. J. van. Infrared Reflectography : A Contribution to the Examination of Earlier European Paintings, Universiteit van Amsterdam, Amsterdam, 1970.
(21) Walmsley, E.; Metzger, C.; Delaney, J. K.; Fletcher, C. Improved Visualization of Underdrawings with Solid-State Detectors Operating in the Infrared. *Studies in Conservation* **1994**, *39* (4), 217–231. https://doi.org/10.1179/sic.1994.39.4.217.
(22) Faries, M. Analytical Capabilities of Infrared Reflectography: An Art Historian's Perspective. In *Scientific Examination of Art: Modern Techniques in Conservation and Analysis, Papers of the Arthur M. Sackler Colloquium of the National Academy of Sciences*; National Academies Press: Washington D.C., 2005; pp 87–104.
(23) Nevin, A. Fluorescence for the Analysis of Paintings. In *Analytical Chemistry for the Study of Paintings and the Detection of Forgeries*; Colombini, M. P., Degano, I., Nevin, A., Eds.; Cultural

Heritage Science; Springer International Publishing: Cham, 2022. https://doi.org/10.1007/978-3-030-86865-9.

(24) Alfeld, M.; Pedroso, J. V.; van Eikema Hommes, M.; Van der Snickt, G.; Tauber, G.; Blaas, J.; Haschke, M.; Erler, K.; Dik, J.; Janssens, K. A Mobile Instrument for in Situ Scanning Macro-XRF Investigation of Historical Paintings. *Journal of Analytical Atomic Spectrometry* **2013**, *28*, 760–767. https://doi.org/10.1039/c3ja30341a.

(25) Alfeld, M.; De Nolf, W.; Cagno, S.; Appel, K.; Siddons, D. P.; Kuczewski, A.; Janssens, K.; Dik, J.; Trentelman, K.; Walton, M.; Sartorius, A. Revealing Hidden Paint Layers in Oil Paintings by Means of Scanning Macro-XRF: A Mock-up Study Based on Rembrandt' s "An Old Man in Military Costume." *J. Anal. At. Spectrom.* **2013**, *28* (1), 40–51. https://doi.org/10.1039/C2JA30119A.

(26) Janssens, K.; Van der Snickt, G.; Vanmeert, F.; Legrand, S.; Nuyts, G.; Alfeld, M.; Monico, L.; Anaf, W.; De Nolf, W.; Vermeulen, M.; Verbeeck, J.; De Wael, K. Non-Invasive and Non-Destructive Examination of Artistic Pigments, Paints, and Paintings by Means of X-Ray Methods. *Topics in Current Chemistry* **2016**, *374* (6), 1–52. https://doi.org/10.1007/s41061-016-0079-2.

(27) Alfeld, M.; de Viguerie, L. Recent Developments in Spectroscopic Imaging Techniques for Historical Paintings - A Review. *Spectrochimica Acta - Part B Atomic Spectroscopy* **2017**, *136*, 81–105. https://doi.org/10.1016/j.sab.2017.08.003.

(28) Vanmeert, F.; De Meyer, S.; Gestels, A.; Avranovich Clerici, E.; Deleu, N.; Legrand, S.; Van Espen, P.; Van Der Snickt, G.; Alfeld, M.; Dik, J.; Monico, L.; De Nolf, W.; Cotte, M.; Gonzalez, V.; Saverwyns, S.; Depuydt-Elbaum, L.; Janssens, K. Non-Invasive and Non-Destructive Examination of Artists' Pigments, Paints and Paintings by Means of X-Ray Imaging Methods. In *Analytical Chemistry for the Study of Paintings and the Detection of Forgeries*; Colombini, M. P., Degano, I., Nevin, A., Eds.; Cultural Heritage Science; Springer International Publishing: Cham, 2022. https://doi.org/10.1007/978-3-030-86865-9.

(29) Trojek, T.; Musílek, L.; Prokeš, R. Depth of Layers in Historical Materials Measurable by X-Ray Fluorescence Analysis. *Radiation Physics and Chemistry* **2019**, *155*, 239–243. https://doi.org/10.1016/j.radphyschem.2018.06.047.

(30) Vanmeert, F.; De Nolf, W.; De Meyer, S.; Dik, J.; Janssens, K. Macroscopic X-Ray Powder Diffraction Scanning, a New Method for Highly Selective Chemical Imaging of Works of Art: Instrument Optimization. *Analytical Chemistry* **2018**, *90* (11), 6436–6444. https://doi.org/10.1021/acs.analchem.8b00240.

(31) Gabrieli, F.; Delaney, J. K.; Erdmann, R. G.; Gonzalez, V.; Loon, A. van; Smulders, P.; Berkeveld, R.; Langh, R. V.; Keune, K. Reflectance Imaging Spectroscopy (RIS) for Operation Night Watch : Challenges and Achievements of Imaging Rembrandt ' s Masterpiece in the Glass Chamber at the Rijksmuseum. *Sensors* **2021**, *21* (6855), 1–18.

(32) Delaney, J. K.; Zeibel, J. G.; Thoury, M.; Littleton, R.; Palmer, M.; Morales, K. M.; de la Rie, E. R.; Hoenigswald, A. Visible and Infrared Imaging Spectroscopy of Picasso's *Harlequin Musician*: Mapping and Identification of Artist Materials *in Situ*. *Applied Spectroscopy* **2010**, *64* (6), 584–594. https://doi.org/10.1366/000370210791414443.

(33) Delaney, J. K.; Thoury, M.; Zeibel, J. G.; Ricciardi, P.; Morales, K. M.; Dooley, K. A. Visible and Infrared Imaging Spectroscopy of Paintings and Improved Reflectography. *Herit Sci* **2016**, *4* (1), 6. https://doi.org/10.1186/s40494-016-0075-4.

(34) Striova, J.; Dal Fovo, A.; Fontana, R. Reflectance Imaging Spectroscopy in Heritage Science. *Riv. Nuovo Cim.* **2020**, *43* (10), 515–566. https://doi.org/10.1007/s40766-020-00011-6.

(35) Delaney, J. K.; Dooley, K. A. Visible and Infrared Reflectance Imaging Spectroscopy of Paintings and Works on Paper. In *Analytical Chemistry for the Study of Paintings and the Detection of Forgeries*; Colombini, M. P., Degano, I., Nevin, A., Eds.; Cultural Heritage Science; Springer International Publishing: Cham, 2022. https://doi.org/10.1007/978-3-030-86865-9.

(36) Vanmeert, F.; De Keyser, N.; Van Loon, A.; Klaassen, L.; Noble, P.; Janssens, K. Transmission

and Reflection Mode Macroscopic X-Ray Powder Diffraction Imaging for the Noninvasive Visualization of Paint Degradation in Still Life Paintings by Jan Davidsz. de Heem. *Analytical Chemistry* **2019**, *91* (11), 7153–7161. https://doi.org/10.1021/acs.analchem.9b00328.

(37) De Nolf, W.; Vanmeert, F.; Janssens, K. *XRDUA* : Crystalline Phase Distribution Maps by Two-Dimensional Scanning and Tomographic (Micro) X-Ray Powder Diffraction. *J Appl Crystallogr* **2014**, *47* (3), 1107–1117. https://doi.org/10.1107/S1600576714008218.

(38) Analytical Approaches to the Analysis of Paintings: An Overview of Methods and Materials. In *Analytical Chemistry for the Study of Paintings and the Detection of Forgeries*; Colombini, M. P., Degano, I., Nevin, A., Eds.; Cultural Heritage Science; Springer International Publishing: Cham, 2022; pp 95–114. https://doi.org/10.1007/978-3-030-86865-9.

(39) Hageraats, S.; Thoury, M.; Cotte, M.; Bertrand, L.; Janssens, K.; Keune, K. Microchemical Imaging of Oil Paint Composition and Degradation: State-of-the- Art and Future Prospects. In *Analytical Chemistry for the Study of Paintings and the Detection of Forgeries*; Colombini, M. P., Degano, I., Nevin, A., Eds.; Cultural Heritage Science; Springer International Publishing: Cham, 2022. https://doi.org/10.1007/978-3-030-86865-9.

(40) Eastaugh, N.; Walsh, V.; Chaplin, T.; Siddall, R. *Pigment Compendium: A Dictionary and Optical Microscopy of Historical Pigments*, 2nd ed.; Butterworth-Heinemann: Oxford, 2008.

(41) Keune, K.; Van Loon, A.; Boon, J. J. SEM Backscattered-Electron Images of Paint Cross Sections as Information Source for the Presence of the Lead White Pigment and Lead-Related Degradation and Migration Phenomena in Oil Paintings. *Microscopy and Microanalysis* **2011**, *17* (5), 696–701. https://doi.org/10.1017/S1431927610094444.

(42) Jaques, V. A. J.; Zikmundová, E.; Holas, J.; Zikmund, T.; Kaiser, J.; Holcová, K. Conductive Cross-Section Preparation of Non-Conductive Painting Micro-Samples for SEM Analysis. *Sci Rep* **2022**, *12* (1), 19650. https://doi.org/10.1038/s41598-022-21882-1.

(43) Goldstein, J. I.; Newbury, D. E.; Michael, J. R.; Ritchie, N. W. M.; Scott, J. H. J.; Joy, D. C. *Scanning Electron Microscopy and X-Ray Microanalysis*; Springer New York: New York, NY, 2018. https://doi.org/10.1007/978-1-4939-6676-9.

(44) Keune, K.; Boon, J. J. Analytical Imaging Studies of Cross-Sections of Paintings Affected by Lead Soap Aggregate Formation. *Studies in Conservation* **2007**, *52* (3), 161–176. https://doi.org/10.1179/sic.2007.52.3.161.

(45) Mazzeo, R.; Joseph, E.; Prati, S.; Millemaggi, A. Attenuated Total Reflection–Fourier Transform Infrared Microspectroscopic Mapping for the Characterisation of Paint Cross-Sections. *Analytica Chimica Acta* **2007**, *599* (1), 107–117. https://doi.org/10.1016/j.aca.2007.07.076.

(46) Spring, M.; Ricci, C.; Peggie, D. A.; Kazarian, S. G. ATR-FTIR Imaging for the Analysis of Organic Materials in Paint Cross Sections: Case Studies on Paint Samples from the National Gallery, London. *Anal Bioanal Chem* **2008**, *392* (1–2), 37–45. https://doi.org/10.1007/s00216-008-2092-y.

(47) Rosi, F.; Cartechini, L.; Sali, D.; Miliani, C. Recent Trends in the Application of Fourier Transform Infrared (FT-IR) Spectroscopy in Heritage Science: From Micro- to Non-Invasive FT-IR. *Physical Sciences Reviews* **2019**, *4* (11). https://doi.org/10.1515/psr-2018-0006.

(48) Liu, G.-L.; Guerreiro, E.; Babington, C.; Kazarian, S. G. ATR-FTIR Spectroscopic Imaging of White Crusts in Cross Sections from Oil Cartoons by Edward Poynter in the Heritage Collections at UK Parliament. *Journal of Cultural Heritage* **2023**, *62*, 251–267. https://doi.org/10.1016/j.culher.2023.05.031.

(49) Gabrieli, F.; Rosi, F.; Vichi, A.; Cartechini, L.; Pensabene Buemi, L.; Kazarian, S. G.; Miliani, C. Revealing the Nature and Distribution of Metal Carboxylates in Jackson Pollock's *Alchemy* (1947) by Micro-Attenuated Total Reflection FT-IR Spectroscopic Imaging. *Anal. Chem.* **2017**, *89* (2), 1283–1289. https://doi.org/10.1021/acs.analchem.6b04065.

(50) Vandenabeele, P.; Edwards, H. G. M.; Moens, L. A Decade of Raman Spectroscopy in Art and Archeology. *Chemical Reviews* **2007**, *107* (3), 675–686. https://doi.org/10.1021/cr068036i.

(51) Rousaki, A.; Vandenabeele, P. Raman Analysis of Inorganic and Organic Pigments. In

Analytical Chemistry for the Study of Paintings and the Detection of Forgeries; Colombini, M. P., Degano, I., Nevin, A., Eds.; Cultural Heritage Science; Springer International Publishing: Cham, 2022. https://doi.org/10.1007/978-3-030-86865-9.

(52) *Analytical Chemistry for the Study of Paintings and the Detection of Forgeries*; Colombini, M. P., Degano, I., Nevin, A., Eds.; Cultural Heritage Science; Springer International Publishing: Cham, 2022. https://doi.org/10.1007/978-3-030-86865-9.

(53) Boon, J. J.; Keune, K.; Van Der Weerd, J.; Geldof, M.; Van Asperen De Boer, J. R. J. Imaging Microspectroscopic, Secondary Ion Mass Spectrometric and Electron Microscopic Studies on Discoloured and Partially Discoloured Smalt in Cross-Sections of 16th Century Paintings. *Chimia* **2001**, *55* (11), 952. https://doi.org/10.2533/chimia.2001.952.

(54) Keune, K.; Boon, J. J. Analytical Imaging Studies Clarifying the Process of the Darkening of Vermilion in Paintings. *Anal. Chem.* **2005**, *77* (15), 4742–4750. https://doi.org/10.1021/ac048158f.

(55) Keune, K.; Hoogland, F.; Boon, J. J.; Peggie, D.; Higgitt, C. Evaluation of the "Added Value" of SIMS: A Mass Spectrometric and Spectroscopic Study of an Unusual Naples Yellow Oil Paint Reconstruction. *International Journal of Mass Spectrometry* **2009**, *284* (1–3), 22–34. https://doi.org/10.1016/j.ijms.2008.10.016.

(56) Alvarez-Martin, A.; Quanico, J.; Scovacricchi, T.; Avranovich Clerici, E.; Baggerman, G.; Janssens, K. Chemical Mapping of the Degradation of Geranium Lake in Paint Cross Sections by MALDI-MSI. *Anal. Chem.* **2023**, *95* (49), 18215–18223. https://doi.org/10.1021/acs.analchem.3c03992.

(57) Krestensen, K. K.; Heeren, R. M. A.; Balluff, B. State-of-the-Art Mass Spectrometry Imaging Applications in Biomedical Research. *Analyst* **2023**, *148* (24), 6161–6187. https://doi.org/10.1039/D3AN01495A.

(58) Bertrand, L.; Robinet, L.; Thoury, M.; Janssens, K.; Cohen, S. X.; Schöder, S. Cultural Heritage and Archaeology Materials Studied by Synchrotron Spectroscopy and Imaging. *Applied Physics A: Materials Science and Processing* **2012**, *106* (2), 377–396. https://doi.org/10.1007/s00339-011-6686-4.

(59) Janssens, K.; Alfeld, M.; Van der Snickt, G.; De Nolf, W.; Vanmeert, F.; Radepont, M.; Monico, L.; Dik, J.; Cotte, M.; Falkenberg, G.; Miliani, C.; Brunetti, B. G. The Use of Synchrotron Radiation for the Characterization of Artists' Pigments and Paintings. *Annual Review of Analytical Chemistry* **2013**, *6* (1), 399–425. https://doi.org/10.1146/annurev-anchem-062012-092702.

(60) Cotte, M.; Susini, J.; Dik, J.; Janssens, K. Synchrotron-Based X-Ray Absorption Spectroscopy for Art Conservation : Looking Back and Looking Forward. *Accounts of Chemical Research* **2010**, *43* (6), 705–714.

(61) Cotte, M.; Genty-Vincent, A.; Janssens, K.; Susini, J. Applications of Synchrotron X-Ray Nano-Probes in the Field of Cultural Heritage. *Comptes Rendus Physique* **2018**, *19* (7), 575–588. https://doi.org/10.1016/j.crhy.2018.07.002.

(62) Bertrand, L.; Cotte, M.; Stampanoni, M.; Thoury, M.; Marone, F.; Schöder, S. Development and Trends in Synchrotron Studies of Ancient and Historical Materials. *Physics Reports* **2012**, *519* (2), 51–96. https://doi.org/10.1016/j.physrep.2012.03.003.

(63) *Photon Source Parameters*. https://www-ssrl.slac.stanford.edu/content/spear3/photon-source-parameters (accessed 2024-08-14).

(64) *PETRA III - Facility Information*. https://photon-science.desy.de/facilities/petra_iii/facility_information/index_eng.html (accessed 2024-08-14).

(65) *THE ACCELERATOR COMPLEX*. https://www.esrf.fr/home/UsersAndScience/Accelerators/the-accelerator-complex.html (accessed 2024-08-14).

(66) Mills, D. M.; Helliwell, J. R.; Kvick, Å.; Ohta, T.; Robinson, I. A.; Authier, A. Report of the Working Group on Synchrotron Radiation Nomenclature – Brightness, Spectral Brightness or Brilliance? *J Synchrotron Rad* **2005**, *12* (3), 385–385. https://doi.org/10.1107/S090904950500796X.

(67) Wiedemann, H. *Particle Accelerator Physics*, Fourth Edition.; Springer Berlin Heidelberg: New York, NY, 2015.
(68) *What is a synchrotron? - Canadian Light Source*. https://www.lightsource.ca/public/what-is-a-synchrotron.php#AboutSynchrotronLight (accessed 2024-08-14).
(69) *What is synchrotron light? - ANSTO*. https://www.ansto.gov.au/education/nuclear-facts/what-is-synchrotron-light (accessed 2024-08-14).
(70) *How does a synchrotron radiation source work?* https://photon-science.desy.de/research/students__teaching/primers/synchrotron_radiation/index_eng.html (accessed 2024-08-14).
(71) *About Synchrotrons - Diamond Light Source*. Diamond. https://www.diamond.ac.uk/Home/About/FAQs/About-Synchrotrons.html (accessed 2024-11-15).
(72) Cotte, M.; Susini, J.; Solé, V. A.; Taniguchi, Y.; Chillida, J.; Checroun, E.; Walter, P. Applications of Synchrotron-Based Micro-Imaging Techniques to the Chemical Analysis of Ancient Paintings. *Journal of Analytical Atomic Spectrometry* **2008**, *23* (6), 820–828. https://doi.org/10.1039/b801358f.
(73) Cotte, M.; Autran, P. O.; Berruyer, C.; Dejoie, C.; Susini, J.; Tafforeau, P. Cultural and Natural Heritage at the ESRF: Looking Back and to the Future. *Synchrotron Radiation News* **2019**, *32* (6), 34–40. https://doi.org/10.1080/08940886.2019.1680213.
(74) Janssens, K.; De Nolf, W.; Van Der Snickt, G.; Vincze, L.; Vekemans, B.; Terzano, R.; Brenker, F. E. Recent Trends in Quantitative Aspects of Microscopic X-Ray Fluorescence Analysis. *TrAC - Trends in Analytical Chemistry* **2010**, *29* (6), 464–478. https://doi.org/10.1016/j.trac.2010.03.003.
(75) Jacobsen, C. X-Ray Spectromicroscopy. In *X-ray Microscopy*; Cambridge University Press, 2019. https://doi.org/10.1017/9781139924542.
(76) Jacobsen, C. X-Ray Physics. In *X-ray Microscopy*; Cambridge University Press, 2019. https://doi.org/10.1017/9781139924542.
(77) Margui, E.; van Grieken, R. *X-Ray Fluorescence Spectrometry and Related Techniques : An Introduction*; Margui, E., Grieken, R. van, Eds.; Momentum Press: New York, 2013.
(78) Szalóki, I.; Török, S. B.; Injuk, J.; Van Grieken, R. E. X-Ray Spectrometry. *Anal. Chem.* **2002**, *74* (12), 2895–2918. https://doi.org/10.1021/ac020241k.
(79) Janssens, K. H. A.; Adams, F. C. V.; Rindby, A. *Microscopic X-Ray Fluorescence Analysis*; Wiley: Chichester, 2000.
(80) *Handbook of Practical X-Ray Fluorescence Analysis*; Beckhoff, B., Kanngießer, B., Langhoff, N., Wedell, R., Wolff, H., Eds.; Springer: Berlin, 2006.
(81) Gonzalez, V.; Wallez, G.; Calligaro, T.; Cotte, M.; De Nolf, W.; Eveno, M.; Ravaud, E.; Menu, M. Synchrotron-Based High Angle Resolution and High Lateral Resolution X-Ray Diffraction: Revealing Lead White Pigment Qualities in Old Masters Paintings. *Analytical Chemistry* **2017**, *89* (24), 13203–13211. https://doi.org/10.1021/acs.analchem.7b02949.
(82) Gonzalez, V.; Cotte, M.; Vanmeert, F.; de Nolf, W.; Janssens, K. X-Ray Diffraction Mapping for Cultural Heritage Science: A Review of Experimental Configurations and Applications. *Chemistry - A European Journal* **2020**, *26* (8), 1703–1719. https://doi.org/10.1002/chem.201903284.
(83) Monico, L.; Janssens, K.; Miliani, C.; Brunetti, B. G.; Vagnini, M.; Vanmeert, F.; Falkenberg, G.; Abakumov, A.; Lu, Y.; Tian, H.; Verbeeck, J.; Radepont, M.; Cotte, M.; Hendriks, E.; Geldof, M.; Van Der Loeff, L.; Salvant, J.; Menu, M. Degradation Process of Lead Chromate in Paintings by Vincent van Gogh Studied by Means of Spectromicroscopic Methods. 3. Synthesis, Characterization, and Detection of Different Crystal Forms of the Chrome Yellow Pigment. *Analytical Chemistry* **2013**, *85* (2), 851–859. https://doi.org/10.1021/ac302158b.
(84) Farges, F.; Cotte, M. X-Ray Absorption Spectroscopy and Cultural Heritage: Highlights and Perspectives. In *X-Ray Absorption and X-Ray Emission Spectroscopy: Theory and Applications*; 2015; Vol. 2–2, pp 609–636. https://doi.org/10.1002/9781118844243.ch21.
(85) Zimmermann, P.; Peredkov, S.; Abdala, P. M.; DeBeer, S.; Tromp, M.; Müller, C.; Van Bokhoven, J. A. Modern X-Ray Spectroscopy: XAS and XES in the Laboratory. *Coordination*

Chemistry Reviews **2020**, *423*, 213466. https://doi.org/10.1016/j.ccr.2020.213466.
(86) Keune, K.; Mass, J.; Meirer, F.; Pottasch, C.; van Loon, A.; Hull, A.; Church, J.; Pouyet, E.; Cotte, M.; Mehta, A. Tracking the Transformation and Transport of Arsenic Sulfide Pigments in Paints: Synchrotron-Based X-Ray Micro-Analyses. *J. Anal. At. Spectrom.* **2015**, *30* (3), 813–827. https://doi.org/10.1039/C4JA00424H.
(87) Keune, K.; Mass, J.; Mehta, A.; Church, J.; Meirer, F. Analytical Imaging Studies of the Migration of Degraded Orpiment, Realgar, and Emerald Green Pigments in Historic Paintings and Related Conservation Issues. *Heritage Science* **2016**, *4* (1), 10. https://doi.org/10.1186/s40494-016-0078-1.
(88) Calvin, S. *XAFS for Everyone*; CRC Press Taylor and Francis Group, 2013.
(89) Newville, M. Fundamentals of XAFS. *Reviews in Mineralogy and Geochemistry* **2014**, *78* (1), 33–74. https://doi.org/10.2138/rmg.2014.78.2.
(90) Joly, Y.; Grenier, S. Theory of X-Ray Absorption Near Edge Structure. In *X-Ray Absorption and X-Ray Emission Spectroscopy*; van Bokhoven, J. A., Lamberti, C., Eds.; John Wiley & Sons, Ltd., 2016; pp 73–97. https://doi.org/10.1002/9781118844243.ch4.
(91) Bleuet, P.; Gergaud, P.; Lemelle, L.; Bleuet, P.; Tucoulou, R.; Cloetens, P.; Susini, J.; Delette, G.; Simionovici, A. 3D Chemical Imaging Based on a Third-Generation Synchrotron Source. *TrAC Trends in Analytical Chemistry* **2010**, *29* (6), 518–527. https://doi.org/10.1016/j.trac.2010.02.011.
(92) Tomography. In *Mathematical Methods in Image Reconstruction*; Natterer, F., Wübbeling, F., Eds.; SIAM monographs on mathematical modeling and computation; Society for Industrial and Applied Mathematics: Philadelphia, 2001; pp 41–62.
(93) *Handbook of Mathematical Methods in Imaging*; Scherzer, O., Ed.; Springer New York: New York, NY, 2015. https://doi.org/10.1007/978-1-4939-0790-8.
(94) Jacobsen, C. X-Ray Tomography. In *X-ray Microscopy*; Cambridge University Press, 2019. https://doi.org/10.1017/9781139924542.
(95) Withers, P. J.; Bouman, C.; Carmignato, S.; Cnudde, V.; Grimaldi, D.; Hagen, C. K.; Maire, E.; Manley, M.; Du Plessis, A.; Stock, S. R. X-Ray Computed Tomography. *Nat Rev Methods Primers* **2021**, *1* (1), 18. https://doi.org/10.1038/s43586-021-00015-4.
(96) Ferreira, E. S. B.; Boon, J. J.; Van Der Horst, J.; Scherrer, N. C.; Marone, F.; Stampanoni, M. 3D Synchrotron X-Ray Microtomography of Paint Samples. In *O3A: Optics for Arts, Architecture, and Archaeology II*; Pezzati, L., Salimbeni, R., Eds.; Munich, Germany, 2009; Vol. 7391, p 73910L. https://doi.org/10.1117/12.827511.
(97) Ma, X.; Beltran, V.; Ramer, G.; Pavlidis, G.; Parkinson, D. Y.; Thoury, M.; Meldrum, T.; Centrone, A.; Berrie, B. H. Revealing the Distribution of Metal Carboxylates in Oil Paint from the Micro- to Nanoscale. *Angew. Chem. Int. Ed.* **2019**, *58* (34), 11652–11656. https://doi.org/10.1002/anie.201903553.
(98) Gervais, C.; Boon, J. J.; Marone, F.; Ferreira, E. S. B. Characterization of Porosity in a 19th Century Painting Ground by Synchrotron Radiation X-Ray Tomography. *Applied Physics A: Materials Science and Processing* **2013**, *111* (1), 31–38. https://doi.org/10.1007/s00339-012-7533-y.
(99) Liu, X.; Di Tullio, V.; Lin, Y. C.; De Andrade, V.; Zhao, C.; Lin, C. H.; Wagner, M.; Zumbulyadis, N.; Dybowski, C.; Centeno, S. A.; Chen-Wiegart, Y. chen K. Nano- to Microscale Three-Dimensional Morphology Relevant to Transport Properties in Reactive Porous Composite Paint Films. *Scientific Reports* **2020**, *10* (1), 1–15. https://doi.org/10.1038/s41598-020-75040-6.
(100) Vanmeert, F.; Vandersnickt, G.; Janssens, K. Plumbonacrite Identified by X-Ray Powder Diffraction Tomography as a Missing Link during Degradation of Red Lead in a van Gogh Painting. *Angewandte Chemie - International Edition* **2015**, *54* (12), 3607–3610. https://doi.org/10.1002/anie.201411691.
(101) Price, S. W. T.; Van Loon, A.; Keune, K.; Parsons, A. D.; Murray, C.; Beale, A. M.; Mosselmans, J. F. W. Unravelling the Spatial Dependency of the Complex Solid-State Chemistry of Pb in

a Paint Micro-Sample from Rembrandt's Homer Using XRD-CT. *Chemical Communications* **2019**, *55* (13), 1931–1934. https://doi.org/10.1039/c8cc09705d.
(102) De Jonge, M. D.; Vogt, S. Hard X-Ray Fluorescence Tomography—an Emerging Tool for Structural Visualization. *Current Opinion in Structural Biology* **2010**, *20* (5), 606–614. https://doi.org/10.1016/j.sbi.2010.09.002.
(103) Kalirai, S.; Boesenberg, U.; Falkenberg, G.; Meirer, F.; Weckhuysen, B. M. X-Ray Fluorescence Tomography of Aged Fluid-Catalytic-Cracking Catalyst Particles Reveals Insight into Metal Deposition Processes. *ChemCatChem* **2015**, *7* (22), 3674–3682. https://doi.org/10.1002/cctc.201500710.
(104) Meirer, F.; Weckhuysen, B. M. Spatial and Temporal Exploration of Heterogeneous Catalysts with Synchrotron Radiation. *Nature Reviews Materials* **2018**, *3* (9), 324–340. https://doi.org/10.1038/s41578-018-0044-5.
(105) Maldanis, L.; Hickman-Lewis, K.; Verezhak, M.; Gueriau, P.; Guizar-Sicairos, M.; Jaqueto, P.; Trindade, R. I. F.; Rossi, A. L.; Berenguer, F.; Westall, F.; Bertrand, L.; Galante, D. Nanoscale 3D Quantitative Imaging of 1.88 Ga Gunflint Microfossils Reveals Novel Insights into Taphonomic and Biogenic Characters. *Scientific Reports* **2020**, *10* (1), 1–9. https://doi.org/10.1038/s41598-020-65176-w.
(106) Deng, J.; Lo, Y. H.; Gallagher-Jones, M.; Chen, S.; Pryor, A.; Jin, Q.; Hong, Y. P.; Nashed, Y. S. G.; Vogt, S.; Miao, J.; Jacobsen, C. Correlative 3D X-Ray Fluorescence and Ptychographic Tomography of Frozen-Hydrated Green Algae. *Science Advances* **2018**, *4* (11), 1–11. https://doi.org/10.1126/sciadv.aau4548.
(107) Bossers, K. W.; Valadian, R.; Zanoni, S.; Smeets, R.; Friederichs, N.; Garrevoet, J.; Meirer, F.; Weckhuysen, B. M. Correlated X-Ray Ptychography and Fluorescence Nano-Tomography on the Fragmentation Behavior of an Individual Catalyst Particle During the Early Stages of Olefin Polymerization. *Journal of the American Chemical Society* **2020**, *142*, 3691–3695. https://doi.org/10.1021/jacs.9b13485.
(108) Bossers, K. W.; Valadian, R.; Garrevoet, J.; van Malderen, S.; Chan, R.; Friederichs, N.; Severn, J.; Wilbers, A.; Zanoni, S.; Jongkind, M. K.; Weckhuysen, B. M.; Meirer, F. Heterogeneity in the Fragmentation of Ziegler Catalyst Particles during Ethylene Polymerization Quantified by X-Ray Nanotomography. *JACS Au* **2021**, *1* (6), 852–864. https://doi.org/10.1021/jacsau.1c00130.
(109) Pfeiffer, F. X-Ray Ptychography. *Nature Photonics* **2018**, *12* (1), 9–17. https://doi.org/10.1038/s41566-017-0072-5.
(110) Jacobsen, C. Coherent Imaging. In *X-ray Microscopy*; Cambridge University Press, 2019. https://doi.org/10.1017/9781139924542.
(111) Thibault, P.; Dierolf, M.; Bunk, O.; Menzel, A.; Pfeiffer, F. Probe Retrieval in Ptychographic Coherent Diffractive Imaging. *Ultramicroscopy* **2009**, *109* (4), 338–343. https://doi.org/10.1016/j.ultramic.2008.12.011.
(112) Dierolf, M.; Menzel, A.; Thibault, P.; Schneider, P.; Kewish, C. M.; Wepf, R.; Bunk, O.; Pfeiffer, F. Ptychographic X-Ray Computed Tomography at the Nanoscale. *Nature* **2010**, *467* (7314), 436–439. https://doi.org/10.1038/nature09419.
(113) Sala, S.; Kuppili, V. S. C.; Chalkidis, S.; Batey, D. J.; Shi, X.; Rau, C.; Thibault, P. Multiscale X-Ray Imaging Using Ptychography. *Journal of Synchrotron Radiation* **2018**, *25* (4), 1214–1221. https://doi.org/10.1107/S1600577518007221.
(114) Feller, R. L. *Artists' Pigments: A Handbook of Their History and Characteristics*; National gallery of art: Washington, 1986; Vol. 1.
(115) Roy, A. *Artists' Pigments: A Handbook of Their History and Characteristics*; National gallery of art: Washington, 1993; Vol. 2.
(116) Fitzhugh, E. W. *Artists' Pigments: A Handbook of Their History and Characteristics*; National gallery of art: Washington, 1997; Vol. 3.
(117) Klöckl, I. *Handbook of Colorants Chemistry, Volume 1: Dyes and Pigments Fundamentals*; Walter de Gruyter GmbH: Berlin/Boston, 2023.

(118) Coccato, A.; Moens, L.; Vandenabeele, P. On the Stability of Mediaeval Inorganic Pigments: A Literature Review of the Effect of Climate, Material Selection, Biological Activity, Analysis and Conservation Treatments. *Herit Sci* **2017**, *5* (1), 12. https://doi.org/10.1186/s40494-017-0125-6.
(119) West Fitzhugh, E. Orpiment and Realgar. In *Artists' Pigments: A Handbook of Their History and Characteristics Volume 3*; West Fitzhugh, E., Ed.; Publishing Office, National Gallery of Art: Washington, 1997; pp 47–80.
(120) Wallert, A. Orpiment and Realgar. *Maltechnik Restauro* **1984**, 45–57.
(121) Gliozzo, E.; Burgio, L. Pigments—Arsenic-Based Yellows and Reds. *Archaeol Anthropol Sci* **2022**, *14* (4), 1–37. https://doi.org/10.1007/s12520-021-01431-z.
(122) De Keyser, N.; van der Snickt, G.; Van Loon, A.; Legrand, S.; Wallert, A.; Janssens, K. Jan Davidsz. de Heem (1606-1684): A Technical Examination of Fruit and Flower Still Lifes Combining MA-XRF Scanning, Cross-Section Analysis and Technical Historical Sources. *Heritage Science* **2017**. https://doi.org/10.1186/s40494-017-0151-4.
(123) De Keyser, N.; Broers, F.; Vanmeert, F.; De Meyer, S.; Gabrieli, F.; Hermens, E.; der Snickt, G. V.; Janssens, K.; Keune, K. Reviving Degraded Colors of Yellow Flowers in 17th Century Still Life Paintings with Macro- and Microscale Chemical Imaging. *Science Advances* **2022**, *8* (23), 1–12. https://doi.org/10.1126/sciadv.abn6344.
(124) Rötter, C.; Grundmann, G.; Richter, M.; Van Loon, A.; Keune, K.; Boersma, A.; Rapp, Klaus. *Auripigment / Orpiment. Studien Zu Dem Mineral Und Den Künstlichen Produkten / Studies on the Mineral and the Artificial Products.*; Schuller, M., Emmerling, E., Nerdinger, W., Eds.; Materialien aus dem Institut für Baugeschichte Kunstgeschichte Restaurierung, Architekturmuseum; Verlag Anton Siegl, Fachbuchhandlung GmbH, München, 2007.
(125) van Loon, A.; Noble, P.; Krekeler, A.; Van der Snickt, G.; Janssens, K.; Abe, Y.; Nakai, I.; Dik, J. Artificial Orpiment, a New Pigment in Rembrandt's Palette. *Heritage Science* **2017**, *5* (1), 26. https://doi.org/10.1186/s40494-017-0138-1.
(126) Vermeulen, M.; Palka, K.; Vlček, M.; Sanyova, J. Study of Dry- and Wet-Process Amorphous Arsenic Sulfides: Synthesis, Raman Reference Spectra, and Identification in Historical Art Materials. *Journal of Raman Spectroscopy* **2019**, *50* (3), 396–406. https://doi.org/10.1002/jrs.5534.
(127) Vermeulen, M.; Nuyts, G.; Sanyova, J.; Vila, A.; Buti, D.; Suuronen, J. P.; Janssens, K. Visualization of As(III) and As(v) Distributions in Degraded Paint Micro-Samples from Baroque- and Rococo-Era Paintings. *Journal of Analytical Atomic Spectrometry* **2016**, *31* (9), 1913–1921. https://doi.org/10.1039/c6ja00134c.
(128) Simoen, J.; De Meyer, S.; Vanmeert, F.; de Keyser, N.; Avranovich, E.; Van der Snickt, G.; Van Loon, A.; Keune, K.; Janssens, K. Combined Micro- and Macro Scale X-Ray Powder Diffraction Mapping of Degraded Orpiment Paint in a 17th Century Still Life Painting by Martinus Nellius. *Heritage Science* **2019**, *7* (1), 1–12. https://doi.org/10.1186/s40494-019-0324-4.
(129) Monico, L.; Prati, S.; Sciutto, G.; Catelli, E.; Romani, A.; Balbas, D. Q.; Li, Z.; De Meyer, S.; Nuyts, G.; Janssens, K.; Cotte, M.; Garrevoet, J.; Falkenberg, G.; Tardillo Suarez, V. I.; Tucoulou, R.; Mazzeo, R. Development of a Multi-Method Analytical Approach Based on the Combination of Synchrotron Radiation X-Ray Micro-Analytical Techniques and Vibrational Micro-Spectroscopy Methods to Unveil the Causes and Mechanism of Darkening of "Fake-Gilded" Decorations in a Cimabue Painting. *Journal of Analytical Atomic Spectrometry* **2022**, No. 37, 114–129. https://doi.org/10.1039/d1ja00271f.
(130) Roberts, A. C.; Ansell, H. G.; Bonardi, M. Pararealgar, a New Polymorph of AsS, from British Columbia. *Canadian Mineralogist* **1980**, *18*, 525–527.
(131) Trentelman, K.; Stodulski, L.; Pavlosky, M. Characterization of Pararealgar and Other Light-Induced Transformation Products from Realgar by Raman Microspectroscopy. *Analytical Chemistry* **1996**, *68* (10), 1755–1761. https://doi.org/10.1021/ac951097o.
(132) Gettens, R. J.; Kühn, H.; Chase, W. T. 3. Lead White. *Studies in Conservation* **1967**, *12* (4),

125–139. https://doi.org/10.1179/sic.1967.013.
(133) Gliozzo, E.; Ionescu, C. Pigments—Lead-Based Whites, Reds, Yellows and Oranges and Their Alteration Phases. *Archaeol Anthropol Sci* **2022**, *14* (1), 17. https://doi.org/10.1007/s12520-021-01407-z.
(134) Stols-Witlox, M. 'The Heaviest and the Whitest':1 Lead White Quality in North Western European Documentary Sources, 1400–1900. *Studying old master paintings: technology and practice* **2011**, 284–294.
(135) Stols-Witlox, M.; Megens, L.; Carlyle, L. 'To Prepare White Excellent…': Reconstructions Investigating the Influence of Washing, Grinding and Decanting of Stack-Process Lead White on Pigment Composition and Particle Size. In *The artist's process: technology and interpretation*; Eyb-Green, S., Townsend, J. H., Clarke, M., Nadolny, J., Kroustallis, S., Eds.; Archetype Publications: London, 2012; pp 112–129.
(136) Gonzalez, V.; Wallez, G.; Calligaro, T.; Gourier, D.; Menu, M. Synthesizing Lead White Pigments by Lead Corrosion: New Insights into the Ancient Manufacturing Processes. *Corrosion Science* **2019**, *146*, 10–17. https://doi.org/10.1016/j.corsci.2018.10.033.
(137) Gonzalez, V.; Cotte, M.; Wallez, G.; van Loon, A.; de Nolf, W.; Eveno, M.; Keune, K.; Noble, P.; Dik, J. Rembrandt's Impasto Deciphered via Identification of Unusual Plumbonacrite by Multi-Modal Synchrotron X-Ray Diffraction. *Angewandte Chemie International Edition* **2019**, *58* (17), 5619–5622. https://doi.org/10.1002/anie.201813105.
(138) De Viguerie, L.; Ducouret, G.; Lequeux, F.; Moutard-Martin, T.; Walter, P. Historical Evolution of Oil Painting Media: A Rheological Study. *C. R. Physique* **2009**, *10* (7), 612–621. https://doi.org/10.1016/j.crhy.2009.08.006.
(139) Cotte, M.; Checroun, E.; De Nolf, W.; Taniguchi, Y.; De Viguerie, L.; Burghammer, M.; Walter, P.; Rivard, C.; Salomé, M.; Janssens, K.; Susini, J. Lead Soaps in Paintings: Friends or Foes? *Studies in Conservation* **2017**, *62* (1), 2–23. https://doi.org/10.1080/00393630.2016.1232529.
(140) Izzo, F. C.; Kratter, M.; Nevin, A.; Zendri, E. A Critical Review on the Analysis of Metal Soaps in Oil Paintings. *ChemistryOpen* **2021**, *10* (9), 904–921. https://doi.org/10.1002/open.202100166.
(141) Noble, P.; Wadum, J.; Groen, K. M.; Heeren, R.; van den Berg, K.-J. Aspects of 17th Century Binding Medium: Inclusions in Rembrandt's Anatomy Lesson of Dr Nicolaes Tulp. *Art et Chimie, la Couleur: Actes du congres* **2000**, 126–129.
(142) Higgitt, C.; Spring, M.; Saunders, D. Pigment-Medium Interactions in Oil Paint Films Containing Red Lead or Lead-Tin Yellow. *National Gallery Technical Bulletin* **2003**, *24*.
(143) Hermans, J. J.; Keune, K.; Van Loon, A.; Iedema, P. D. The Crystallization of Metal Soaps and Fatty Acids in Oil Paint Model Systems. *Physical Chemistry Chemical Physics* **2016**, *18* (16), 10896–10905. https://doi.org/10.1039/c6cp00487c.
(144) Boon, J. J., van der Weerd, J., Keune, K., Noble, P., & Wadum, J. Mechanical and Chemical Changes in Old Master Paintings: Dissolution, Metal Soap Formation and Remineralisation Processes in Lead Pigmented Ground/Intermediate Paint Layers of 17th Century Paintings; Rio de Janeiro, 2002; Vol. II, pp 401–406.
(145) van Loon, A.; Vandivere, A.; Delaney, J. K.; Dooley, K. A.; De Meyer, S.; Vanmeert, F.; Gonzalez, V.; Janssens, K.; Leonhardt, E.; Haswell, R.; de Groot, S.; D'Imporzano, P.; Davies, G. R. Beauty Is Skin Deep: The Skin Tones of Vermeer's Girl with a Pearl Earring. *Heritage Science* **2019**, *7* (1), 1–20. https://doi.org/10.1186/s40494-019-0344-0.
(146) De Meyer, S.; Vanmeert, F.; Vertongen, R.; van Loon, A.; Gonzalez, V.; van der Snickt, G.; Vandivere, A.; Janssens, K. Imaging Secondary Reaction Products at the Surface of Vermeer's Girl with the Pearl Earring by Means of Macroscopic X-Ray Powder Diffraction Scanning. *Heritage Science* **2019**, *7* (1), 1–11. https://doi.org/10.1186/s40494-019-0309-3.
(147) Kirby, J.; Spring, M.; Higgitt, C. The Technology of Red Lake Pigment Manufacture: Study of the Dyestuff Substrate. *National Gallery Technical Bulletin* **2005**, *26*.
(148) Gonzalez, V.; Fazlic, I.; Cotte, M.; Vanmeert, F.; Gestels, A.; De Meyer, S.; Broers, F.; Hermans, J.; van Loon, A.; Janssens, K.; Noble, P.; Keune, K. Lead(II) Formate in Rembrandt's *Night*

Watch : Detection and Distribution from the Macro- to the Micro-scale. *Angew Chem Int Ed* **2023**. https://doi.org/10.1002/anie.202216478.
(149) Vermeulen, M.; Sanyova, J.; Janssens, K.; Nuyts, G.; De Meyer, S.; De Wael, K. The Darkening of Copper- or Lead-Based Pigments Explained by a Structural Modification of Natural Orpiment: A Spectroscopic and Electrochemical Study. *Journal of Analytical Atomic Spectrometry* **2017**, *32* (7), 1331–1341. https://doi.org/10.1039/c7ja00047b.
(150) Mühlethaler, B.; Thissen, J. Smalt. *Studies in Conservation* **1969**, *14* (2), 47–61.
(151) Mühlethaler, B.; Thissen, J. Smalt. In *Artists' pigments: a handbook of their history and characteristics*; National gallery of art: Washington, 1993; Vol. 2, pp 111–130.
(152) Cavallo, G.; Riccardi, M. P. Glass-Based Pigments in Painting: Smalt Blue and Lead–Tin Yellow Type II. *Archaeol Anthropol Sci* **2021**, *13* (11), 199. https://doi.org/10.1007/s12520-021-01453-7.
(153) Machado, A.; Vilarigues, M. Blue Enamel Pigment—Chemical and Morphological Characterization of Its Corrosion Process. *Corrosion Science* **2018**, *139*, 235–242. https://doi.org/10.1016/j.corsci.2018.05.005.
(154) Tyler, M. J. Aspects of the Manufacture, Trade and History of Smalt, 2019.
(155) Tite, M. S.; Shortland, A.; Maniatis, Y.; Kavoussanaki, D.; Harris, S. A. The Composition of the Soda-Rich and Mixed Alkali Plant Ashes Used in the Production of Glass. *Journal of Archaeological Science* **2006**, *33* (9), 1284–1292. https://doi.org/10.1016/j.jas.2006.01.004.
(156) Spring, M. Colourless Powdered Glass as an Additive in Fifteenth- and Sixteenth-Century European Paintings. *National Gallery Technical Bulletin* **2012**, *33*, 4–26.
(157) Plesters, J. A Preliminary Note on the Incidence of Discolouration of Smalt in Oil Media. *Studies in Conservation* **1969**, *14* (2), 62–74.
(158) Giovanoli, R.; Mühlethaler, B. Investigation of Discoloured Smalt. *Studies in Conservation* **1970**, *15* (1), 37–44.
(159) Noble, P.; van Loon, A. New Insights into Rembrandt's Susanna, Changes of Format, Smalt Discolouration, Identification of Vivianite, Fading of Yellow and Red Lakes, Lead White Paint. *Art Matters-Netherlands Technical Studies in Art* **2005**, *2*, 76–96.
(160) Espinosa Pesqueira, M. E.; Lemus, E. A. The Use of Smalt in Simon Pereyns Panel Paintings: Intentional Use and Color Changes. *MRS Proc.* **2014**, *1618*, 131–139. https://doi.org/10.1557/opl.2014.462.
(161) Robinet, L.; Spring, M.; Pagès-Camagna, S.; Vantelon, D.; Trcera, N. Investigation of the Discoloration of Smalt Pigment in Historic Paintings by Micro-X-Ray Absorption Spectroscopy at the Co K-Edge. *Anal. Chem.* **2011**, *83* (13), 5145–5152. https://doi.org/10.1021/ac200184f.
(162) Bikker, J. *The Night Watch*; Rijksmuseum: Amsterdam, 2013.
(163) Bruyn, J. The "Night Watch", or Officers and Men of the Company of Captain Frans Banning Cocq and Lieutenant Willem van Ruytenburgh. In *A corpus of Rembrandt paintings III*; M. Nijhoff: Dordrecht, 1989; pp 430–485.
(164) van Duijn, E.; Kok, J. P. F. The Restorations of Rembrandt's "Night Watch." In *The Art of Conservation*; Martineau, J., Bomford, D., Eds.; The Burlington Press: London, 2023; Vol. 158, pp 268–303.
(165) Duijn, E. V. 'Like a Drunkard, the Diseased Painting Craved the Regenerating Alcohol...' The Numerous Varnish Treatments of Rembrandt's 'Night Watch' between 1889 and 1936. In *Postprints for the Rembrandt Conservation Histories*; Archetype London/Rijksmuseum Amsterdam, 2021.
(166) Duijn, E. V. ICOM-CC ' As Much as Is Necessary for the Harmony of the Picture Not to Be Disturbed ': The Materials and Methods Used during the 1945 – 47 Treatment of The Night Watch by Rembrandt. **2021**, No. June 1945, 1–7.
(167) Thiel, L. Damaging and Restoration Night Watch. *Bulletin van het Rijksmuseum* **1976**, *24* (1/2), 4–13.
(168) van de Wetering, E.; Groen, C. M.; Mosk, J. A. Summary Report on the Results of the

Technical Examination of Rembrandt's Night Watch. *Bulletin van het Rijksmuseum* **1976**, *24* (1/2), 68–98.
(169) Groen, K.; Wetering, E. van de. Grounds in Rembrandt's Workshop and in Paintings by His Contemporaries. In *A Corpus of Rembrandt Paintings IV*; Stichting Foundation Rembrandt Research Project: Dordrecht, 2005; pp 318–334 and 660–677.
(170) Groen, K. Earth Matters. The Origin of the Material Used for the Preparation of the Night Watch and Many Other Canvases in Rembrandt's Workshop after 1640. *ARTMATTERS - Netherlands Technical Studies in Art* **2005**, *3*, 138–154.
(171) *Operation Night Watch*. https://www.rijksmuseum.nl/en/whats-on/exhibitions/operation-night-watch.
(172) Erdmann, R. G. *717 gigapixel visible light composite image (5 µm resolution) for Rembrandt's Night Watch*. https://images.erdmann.io/curtain.html?prefix=Rijksmuseum/SK-C-5/&pointer=0.562,0.004&i=SK-C-5_VIS_5-um_2020-09-08[l=VIS%205%20µm].